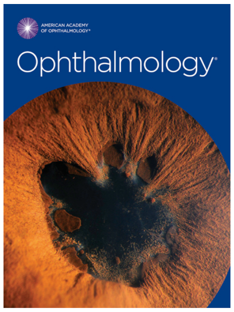

The Oculome panel test: next-generation sequencing to diagnose a diverse range of genetic developmental eye disorders

Aara Patel, Jane D. Hayward, Vijay Tailor, Rodney Nyanhete, Helena Ahlfors, Camila Gabriel, Tommaso B. Jannini, Yassir Abbou-Rayyah, Robert Henderson, Ken K. Nischal, Lily Islam, Maria Bitner-Glindzicz, Jane Hurst, Leonardo E. Valdivia, Mario Zanolli, Mariya Moosajee, John Brookes, Maria Papadopoulos, Peng T. Khaw, Thomas Cullup, Lucy Jenkins, Annegret Dahlmann-Noor, Jane C. Sowden

PII: S0161-6420(18)31858-X
DOI: https://doi.org/10.1016/j.ophtha.2018.12.050
Reference: OPHTHA 10632

To appear in: *Ophthalmology*

Received Date: 3 August 2018
Revised Date: 18 December 2018
Accepted Date: 21 December 2018

Please cite this article as: Patel A, Hayward JD, Tailor V, Nyanhete R, Ahlfors H, Gabriel C, Jannini TB, Abbou-Rayyah Y, Henderson R, Nischal KK, Islam L, Bitner-Glindzicz M, Hurst J, Valdivia LE, Zanolli M, Moosajee M, Brookes J, Papadopoulos M, Khaw PT, Cullup T, Jenkins L, Dahlmann-Noor A, Sowden JC, The Oculome panel test: next-generation sequencing to diagnose a diverse range of genetic developmental eye disorders, *Ophthalmology* (2019), doi: https://doi.org/10.1016/j.ophtha.2018.12.050.

Title

The Oculome panel test: next-generation sequencing to diagnose a diverse range of genetic developmental eye disorders

Running Title

Genetic testing of developmental eye disorders

Authors

Aara Patel[1 †], Jane D Hayward[1 †], Vijay Tailor[2], Rodney Nyanhete[3], Helena Ahlfors[3], Camila Gabriel[1], Tommaso B Jannini[1], Yassir Abbou-Rayyah[4], Robert Henderson[4], Ken K. Nischal[4,5], Lily Islam[1,6], Maria Bitner-Glindzicz[1], Jane Hurst[1], Leonardo E. Valdivia[7], Mario Zanolli[8], Mariya Moosajee[2, 4], John Brookes[4, 9], Maria Papadopoulos[9], Peng T Khaw[2,9], Thomas Cullup [3], Lucy Jenkins[1, 3], Annegret Dahlmann-Noor[2], Jane C Sowden[1*]

1. UCL Great Ormond Street Institute of Child Health, and NIHR Biomedical Research Centre at Great Ormond Street Hospital for Children NHS Foundation Trust and University College London, London, UK

2. NIHR Biomedical Research Centre at Moorfields Eye Hospital NHS Foundation Trust, and UCL Institute of Ophthalmology London, UK

3. North East Thames Regional Genetics Laboratory, Great Ormond Street Hospital for Children NHS Trust, London, UK

4. Department of Ophthalmology, Great Ormond Street Hospital for Children NHS Trust, London, UK

5. UPMC Eye Center, Children's Hospital of Pittsburgh of UPMC, University of Pittsburgh School of Medicine, Pittsburgh, PA, USA.

6. Birmingham Women’s Hospital, Birmingham, UK

7. Centre for Integrative Biology, Facultad de Ciencias, Universidad Mayor, Santiago, Chile

8. Facultad de Medicina Clínica Alemana de Santiago – Universidad del Desarrollo, Santiago, Chile

9. Glaucoma Service, Moorfields Eye Hospital NHS Foundation Trust, London, UK

† These authors contributed equally to this work

*Correspondence: Professor Jane C. Sowden, PhD: j.sowden@ucl.ac.uk, Birth Defects Research Centre, Stem Cells and Regenerative Medicine Section, UCL Great Ormond Street Institute of Child Health, 30 Guilford Street, London, WC1N 1EH UK, Tel: +44 (0) 20 7905 2121, Fax: +44 (0) 20 7831 4366

Conflict of Interest: None

Key words: microphthalmia, coloboma, anterior segment dysgenesis, congenital glaucoma, congenital cataracts, retinal dystrophies, genetics, developmental, childhood, paediatric ophthalmology

Abstract (346 words)

Purpose: To develop a comprehensive next-generation sequencing panel assay which screens genes known to cause developmental eye disorders and inherited eye disease (Oculome test) and to evaluate its diagnostic yield in a paediatric cohort with malformations of the globe, anterior segment anomalies and/or childhood glaucoma.

Design: Evaluation of diagnostic test.

Participants: 277 children age 0-16 years diagnosed with nonsyndromic or syndromic developmental eye defects without a genetic diagnosis.

Methods: We developed a new Oculome panel using a custom-designed Agilent SureSelect QXT target capture method to capture and perform parallel high through put sequencing analysis of 429 genes associated with eye disorders. We confirmed suspected pathogenic variants by bidirectional Sanger sequencing.

Main outcome measures: We collated clinical details and the oculome molecular genetic results.

Results: The Oculome design covers 429 known eye disease genes; these are subdivided into 5 overlapping virtual sub-panels for anterior segment developmental anomalies and glaucoma (ASDA; 59 genes), microphthalmia-anophthalmia-coloboma (MAC; 86 genes), congenital cataracts and lens-associated conditions (CAT; 70 genes), retinal dystrophies (RET; 235 genes), and albinism (15 genes), and as well as additional genes implicated in optic atrophy and complex strabismus (10 genes). Panel development and testing included analysing n = 277 clinical samples and 3 positive control samples using Illumina sequencing platforms; >30 X read-depth was achieved for 99.5% of the targeted 1.77 Mb region. Bioinformatics analysis performed using a pipeline based on Freebayes and ExomeDepth to identify coding sequence and copy number variants respectively, resulted in a definitive diagnosis in 68 / 277 cases with variability in diagnostic yield between phenotypic sub-groups; MAC: 8.2% (8 of 98 cases solved), ASDA: 24.8% (28 of 113 cases solved), other / syndromic 37.5% (3 of 8 cases solved); RET: 42.8% (21 of 49 cases solved); CAT: 88.9% (8 of 9 cases solved). **Conclusion**: The Oculome test diagnoses a comprehensive range of genetic conditions affecting the development of the eye, potentially replacing protracted and costly multidisciplinary assessments and allowing for faster targeted management. The Oculome enabled the molecular

diagnosis of a significant number of cases in our sample cohort of varied ocular birth defects.

Introduction

An estimated 1.4 million children are blind. [1] The incidence of childhood blindness ranges from 0.3-0.4 per 1000 in developed countries to 1.2 per 1000 in undeveloped countries. [2] In all countries, childhood blindness occurs as a result of congenital and developmental abnormalities. In the UK developmental eye defects resulting in severe visual impairment or blindness affect 4 in 10,000 children each year. Microphthalmia, anophthalmia and coloboma (MAC) affect an estimated 1.19 per 10,000 children by the age of 16 years, [3] congenital glaucoma affects 1 in 20,000 children [4]; approximately 3 in 10,000 children under 15 years old are affected by congenital cataracts [5]; retinal dystrophies affect 2.2 in 10,000 children by the age of 16, with retinitis pigmentosa being the most common retinal dystrophy [6, 7]; albinism has a global prevalence of 1 in 20,000. [8] Although these developmental disorders are individually rare, they collectively account for a significant proportion of global blindness. The proportion due to genetic causes is unresolved.

Molecular diagnoses are largely unavailable for children with developmental eye disorders due to the genetic heterogeneity of these conditions, the limited availability of multi-gene panel tests and the low level of diagnosis achieved by sequential screening of individual candidate genes. Next generation sequencing (NGS) is a more cost-effective method to provide a genetic diagnosis in a wide range of congenital and developmental conditions. [9-13] Whilst genetic panel tests are available for some eye conditions, notably retinal dystrophies and congenital cataract, [13-16] comprehensive panel assays are not available for a wide range of conditions affecting the development of the anterior segment and whole globe, such as congenital or juvenile glaucoma, anterior segment dysgenesis, MAC, optic atrophy and nystagmus. A molecular diagnosis of the genetic changes underlying MAC and anterior segment developmental anomalies (ASDA) is particularly challenging, as these conditions have highly heterogeneous presentations and diverse genetic causes. Many developmental eye disorders form part of a syndrome involving additional metabolic, developmental, physical or sensory abnormalities. These can be difficult to define and may be missed if children are examined solely by an ophthalmologist. Panels that allow for simultaneous testing of a large number of genes are particularly attractive for phenotypically diverse and sometimes overlapping conditions.

We aimed to develop a single comprehensive test, which would provide a molecular diagnosis of a wide range of conditions of developmental eye defects. We grouped genes into virtual subpanels to evaluate a narrower gene range where necessary. The full panel maximises the potential for differential diagnosis without the need for multiple testing. This study included two phases: we developed the new NGS multi-gene panel assay (Oculome), including human genes with a known Mendelian disease association and then evaluated the diagnostic yield of the Oculome test in 277 undiagnosed children. We achieved a significant diagnostic yield over all phenotypic sub-groups screened. The Oculome multi-gene test addresses the specific challenge of high genetic and phenotypic heterogeneity in molecular diagnosis for developmental eye conditions by providing high throughput screening of individuals with diverse ocular phenotypes using the same capture panel.

Methods

Participants and genomic DNA sample preparation

The study was approved by the National Research Ethics Committee London-Dulwich (11/LO/1243) and registered on the National Institute of Health Research Portfolio, ID 11800, Childhood blindness: genetic diagnosis for clinical management. It adhered to the tenets of the Declaration of Helsinki.

Unrelated children, age 0-16 years, with developmental eye defects and no previous genetic diagnosis, who attended clinics at Moorfields Eye Hospital and Great Ormond Street Hospital for Children, London, UK were recruited. DNA from 7 families was also analysed from collaborating centres in Italy and Chile. Consent was obtained from parents or guardians of patients. Age-appropriate written information material was provided; any questions were addressed before obtaining written consent and assent. Age at study participation, family history, gender and ethnic background was recorded. From the medical notes, ocular and systemic diagnoses, age at diagnosis of the eye condition, and best-corrected visual acuity (BCVA) with both eyes open in logMAR on the day of study participation was recorded. Where visual acuity was recorded as “counting fingers”, a BCVA of 2.1 logMAR was noted, for “hand movements only” 2.4 logMAR, for “perception of light” 2.7 logMAR, and for “no perception of light” or “ocular prosthesis/artificial eye”, 3 logMAR. [17]. Widefield colour and autofluorescence retinal imaging was performed with Optos California (Optos PLC, Scotland UK); macular photography was performed with Topcon fundus camera (Topcon) and OCT imaging was obtained with the Heidelberg Spectralis (Heidelberg Inc, Germany).

A peripheral blood sample was obtained where possible, or saliva if not, from the child, parents and siblings (the latter for co-segregation analysis). The chemagic STAR DNA Blood4k Kit, with a sample volume 2-4ml, following manufacturer’s protocols was used to extract gDNA. Saliva was collected and gDNA extracted using the standard protocol of the Oragene DNA (OG500) collection kit.

Target capture, library preparation and next generation sequencing

A custom SureSelect target capture kit (Agilent Technologies, Santa Clara, CA) was designed to include coding exons plus a flanking region of 25 bases into introns upstream and downstream for known developmental eye disorder and ocular genetic disease genes using the Agilent Technologies eArray tool. The genes were identified using OMIM, RetNet, and published literature. Two design iterations were evaluated. Based on evaluation of oculome design Version 1, a second design iteration, Version 2, was prepared including additional capture baits in regions found to have low, or no, coverage from the first sequencing run. Additional genes were added to the second iteration to provide comprehensive coverage of genes known to cause Mendelian ocular disorders. Boosting was achieved using the Agilent eArray tool advanced design features. Both iterations covered the same 387 genes and iteration 2 covered an additional 42 genes giving a total of 429 genes. The 1.77 Mb genomic capture design can be accessed at https://earray.chem.agilent.com/suredesign.

Fragmented genomic DNA sequencing libraries were prepared using the Agilent SureSelect QXT method, which employs a transposase to simultaneously fragment and adapter tag DNA samples using an input of 50ng of total gDNA. 8 cycles of pre-amplification PCR were performed following library preparation and these were run on an Agilent Bioanalyzer DNA1000 chip to check library size (~300-350 bp) and to calculate DNA concentration for hybridisation to capture baits. Between 500ng and 750ng of pre-capture library was then added for hybridisation to the capture 120mer cRNA probes specific for regions of interest. A final amplification of 12 cycles of PCR was performed to add sample specific indices and produce final libraries. The Agilent Tapestation was used to assess the quality of each library. Finally libraries were diluted and pooled at 10nM concentrations. Those for a MiSeq run were diluted to 12pM, for a HiSeq run to 8pM and for a NextSeq run to 1.3pM. Longer read lengths and larger fragments produced by the SureSelect QXT method boosted coverage.

In total 277 patient samples were successfully interrogated using Illumina sequencing platforms (see Table 1); 88 samples on iteration 1 and 166 on iteration 2 of the oculome.

Bioinformatics analysis pipeline

For the pilot run of 8 samples, variant calling was done using VarScan2 (VarScan2 v2.3.6: http://varscan.sourceforge.net/) and variant annotation using VEP (Variant effect predictor v73: http://www.ensembl.org/info/docs/tools/vep/index.html). All subsequent analyses were conducted using an updated pipeline of open-source tools, BWA (Burrows Wheeler Aligner v0.6.1-r104: http://bio-bwa.sourceforge.net/) for read alignment, SamTools (Samtools v0.1.18: http://samtools.sourceforge.net/) for pileup Freebayes for variant calling and VEP (Variant effect predictor v73: http://www.ensembl.org/info/docs/tools/vep/index.html/ and Alamut batch: http://www.interactive-biosoftware.com/alamut-batch/) for variant annotation.

Pipeline output was limited to variants in coding exons +/- 20bp. Variants had to be present in 20% of at least 30 reads to be called. Further filtering excluded variants present at 2% or greater in the Exome Variant Server (EVS) or 1000 genomes datasets (Class I variants). Variants were classified using a five-class system consistent with the American College of Medical Genetics and Genomics (ACMG) standards and guidelines for the interpretation of sequence variants [18] with Class 2 being likely benign variants and Class 5 being previously reported pathogenic variants relevant to the phenotype of the patient. The classification system is described in detail in Figure 2.

Copy Number Variation (CNV) analysis was developed and performed using a pipeline based on the algorithm ExomeDepth [19] for all samples. Briefly, numbers of reads aligning to each exon in the target region in each individual were compared to an aggregate reference set composed of other samples within the same run to identify exons with significantly higher or significantly lower read counts indicating a duplication or deletion. CNV variant calls were then filtered against the Conrad database of common CNVs. [20]

Sanger sequencing

Sanger sequencing was performed of predicted class 4 and 5 variants; Class 3 variants of uncertain significance in a gene relevant to the clinical phenotype were also evaluated using Sanger sequencing. This included sequencing in affected and unaffected family members (where possible) to confirm co-segregation of predicted mutations with disease. Primer3 software (version 0.4.0 http://frodo.wi.mit.edu/primer3/) was used to design primers for Sanger sequencing. A 200-400 base pair product surrounding the variant was amplified using a standard polymerase chain reaction prior to sequencing and separation by capillary electrophoresis using the ABI 3730XL (Applied Biosystems, Carlsbad, CA).

Results

We developed a multi-gene high throughput sequencing panel test, the Oculome panel test, to aid genetic diagnosis of childhood eye conditions. The Oculome panel design aimed to provide comprehensive coverage of known developmental eye disorder and inherited eye disease genes. Only human genes with a known association to monogenic eye disease were selected, including syndromic conditions that include ocular phenotypes. Most are listed in OMIM except for the most recently identified genes. Genes that have been identified only in animal models of eye disease were not included. Figure 1 A and Supplementary Table 1 detail the 429 genes in five overlapping virtual sub panels according to phenotypic category.

The sub-panels are organised in relation to the affected region of the eye: anterior segment dysgenesis and glaucoma (ASDA; n = 59), microphthalmia-anophthalmia-coloboma (MAC; n = 86), congenital cataracts and lens-associated (CAT; n = 70), retinal dystrophies (RET; n = 235), and albinism (n = 15) as well as additional genes implicated in optic atrophy (n =11) and complex strabismus n= 10 (See Supplementary Table 1 for gene lists and details of associated phenotypes). The CAT sub-panel covers genes associated with isolated and syndromic forms of cataract as well as lens phenotypes, such as ectopia lentis. The ASDA sub-panel covers genes associated with anterior segment developmental anomalies, such as aniridia, Axenfeld-Rieger syndrome, congenital glaucoma, iridogoniodysgenesis, Peter's anomaly and corneal dystrophies. Genes causing Mendelian glaucoma are included in the ASDA subpanel as there is considerable overlap between the causal genes of the two phenotypes. [21-23] The MAC sub-panel covers genes associated with isolated or syndromic microphthalmia, anophthalmia and ocular coloboma as well as other whole globe defects such as nanophthalmia (small posterior segment only), macrophthalmia (increased eye size); 63% of genes in this sub-panel are associated with a syndromic phenotype. The RET subpanel covers known inherited retinal disease and includes those affecting rod or cone photoreceptor cells, retinal pigment epithelium (RPE) and stationary or progressive disease, as well as those with extra-ocular phenotypes (syndromic). [24] The albinism panel covers genes associated with syndromic and non-syndromic ocular and oculocutaneous sub-types of albinism involving defects in pigmentation as well as nystagmus, photophobia, reduced visual acuity and strabismus. Genes are included in more than one sub-panel when they are reported to cause more than one phenotype; a Venn diagram (Figure 1A) indicates the number of genes that cause phenotypes in more than one phenotypic sub-group (Supplementary Table 1). Around 56% of all genes on the Oculome are associated with extra ocular phenotypes.

To assess efficacy of the oculome multi-gene panel test a total of 277 children without genetic diagnosis for their eye condition were recruited to the study for sequence analysis (Figure 1 B). Of the individuals included in the analysis 42 % (n= 114) were female. A proportion (16 %, n= 45) of subjects were reported to have extra-ocular signs and symptoms consistent with a syndromic phenotype. At least 9 different ethnicities were represented. 19 %, (n = 52) reported a family history. Based on medical notes at the time of recruitment, the participants were grouped according to phenotype. The largest phenotypic groups were recorded as having paediatric glaucoma and / or anterior segment developmental anomalies (ASDA) phenotype (40.7%; n= 113), or disorders of the globe (MAC) (35.4 %; n= 98). Smaller groups of children presenting with early onset retinal dystrophies (17.7%; n= 49), cataract (3.2%; n= 9) and undiagnosed syndromic conditions (2.9%; n=8), including one case of ocular albinism, were recruited allowing comparison of diagnostic yields between phenotypic groups (Figure 1 B).

Oculome panel assay design and development

In the pilot study analysing 8 DNA samples on Oculome design V1, coverage of 96% of the target region over 30X was achieved. Three of these samples were positive controls from individuals with a known genetic diagnosis including a whole gene deletion in *FOXC1*, digenic mutations in *FOXC1* and *PITX2* and a mutation in *FOXE3* [25-27]. All four mutations were successfully identified in the Oculome test. A homozygous frameshift variant in *RDH12* was identified in one of the other five undiagnosed cases consistent with a diagnosis of Leber's congenital amaurosis (Case 7). Re-design of the SureSelect targets improved coverage from to 99.5% >30X for Oculome design V2 across coding exons of 429 genes. Excellent quality metrics were obtained with cluster densities ranging between 800-900K/mm2 and 94% passing filter (PF). Table 1 shows details of quality metrics, including coverage and mean depth for each of the six Illumina sequencing runs performed to screen

DNA samples from the 277 participants in the study. Coverage graphs are shown in Supplementary Figure 1.

Diagnostic utility in children with unknown molecular diagnoses

Variants were interpreted and classified into five classes, in accordance with ACMG guidelines [18] as detailed in Figure 2. Predicted or known pathogenic mutations (class 4 or 5 variants) relevant to the phenotype were identified in 68 samples after Oculome panel testing giving an overall diagnostic yield of 24.5% (Table 2).

37 cases had recessive mutations (homozygous and compound heterozygous), 27 dominant, 3 were X-linked and 1 composite. Sanger sequencing was used to validate class 4 and 5 in 25 of the 68 individuals. All variants investigated were confirmed. In addition, segregation analysis in relatives was possible for 20 of these cases. In all cases the variants segregated with the phenotype, except Case 190. Here, the variant in *GDF3,* although previously reported as pathogenic, was detected in the apparently unaffected father. While it cannot be ruled out that the father has a mild subclinical phenotype, our findings were consistent with previous reports of reduced penetrance, [28] as well as variable expressivity (ocular or skeletal phenotypes or both) for this variant. [29] We calculated the diagnostic yield for each sub-panel as the proportion of patients screened within the four phenotypic groups (anterior segment dysgenesis and glaucoma, MAC, early onset retinal dystrophies, congenital cataract) that were detected with a positive class 4 or 5 mutation. Diagnostic yield between phenotypic sub-panels was found to be variable. Table 2 lists the diagnostic yield for each phenotypic grouping. Table 3 describes all class 4 and 5 mutations detected, arranged according to each sub-panel that contained at least one pathogenic mutation. Supplementary Table 2 shows phenotypic information for cases with class 4 and 5 variants.

Molecular diagnosis per phenotypic subgroup

Microphthalmia, Anophthalmia and Coloboma (MAC) The MAC spectrum of microphthalmia (small eyes), anophthalmia (absent eyes) and ocular coloboma (abnormality in optic fissure closure) is known to be phenotypically heterogeneous often presenting with only one eye affected [30, 31] and in combination with other ocular features. In this study 98 MAC cases were screened (Figure 3 A-C). 37.5% (n = 36 cases) had a fissure closure defect. The remainder were reported as either only microphthalmia or anophthalmia. 39.6% (38 cases) had a bilateral eye phenotype, 56.2% (54 cases) had a unilateral phenotype. Some cases also had another eye defect such as anterior segment dysgenesis, cataract, PHPV (Persistent Hyperplastic Primary Vitreous) or a retinal anomaly. 20.8% (20 cases) had syndromic features Figure 3 A – C). 8 cases were known to have a relative with the same phenotype or consanguineous parents.

Class 4/5 pathogenic variants were detected in 8 cases (8.2 %) in eight different genes with dominant heterozygous, recessive compound heterozygous and X-linked genotypes (Table 3).

Two of these cases (Case 25 and 112) were patients with bilateral anophthalmia and both had mutations in genes involved in the metabolism of retinoic acid (*ALDH1A3* and *STRA6*). [32-34] The variants in *ALDH1A3* were both novel missense variants, were biallelic and were both present in the similarly affected sibling of the proband (Case 25; Figure 4A). Of the variants in *STRA6*, one was inherited from the mother; the father was unavailable for study (Case 112; Figure 4B). Case 12 with coloboma, microphthalmia and syndactyly was found to have pathogenic variants in *SMOC1*, a gene implicated in ophthalmo-acromelic syndrome [35, 36] (Figure 4C). Two cases with unilateral microphthalmos had pathogenic variants in *GDF3* and *GDF6*. The variant in *GDF3*, identified in Case 190 with microphthalmia and skeletal defects, was inherited from his apparently unaffected father (Figure 4D). It has been reported previously in three families with Klippel-Fleil syndrome [29] with variable phenotypes and reduces the levels of mature *GDF3* synthesized. It is possible that the father has a subclinical phenotype. The variant in *GDF6*, identified in Case 208 with isolated microphthalmia, had previously been reported in patients with isolated microphthalmia and syndromic coloboma. [37] In this case segregation analysis was not possible. Case 260, diagnosed with macular folds and congested optic nerves was found to have a homozygous, likely pathogenic missense variant in *PRSS56*, confirming a diagnosis of nanophthalmos (posterior microphthalmos) [38] (Figure 4E).

Case 294, diagnosed with microphthalmia and possible Gorlin-Goltz syndrome, had a pathogenic heterozygous missense variant in *PORCN*. The variant had previously been implicated in two individuals with Focal Dermal Hypoplasia (OMIM: 305600), a multisystem disorder with an X-linked dominant mode of inheritance. [39] Segregation analysis showed that it occurred *de-novo* (Figure 4F).

Finally, Case 10, diagnosed with unilateral microphthalmia and bilateral ASDA was found to have a *de-novo* frameshift mutation in *FOXC1*, a major causative gene for anterior segment malformation (Iridogoniodysgenesis and Axenfeld-Rieger syndrome), illustrating the phenotypic heterogeneity in eye malformations (Figure 4G). The same individual also carried a missense variant (see Table 3) in *FOXC1* previously associated with a mild iridogoniodysgenesis phenotype. [40]

In this comprehensive screening of MAC cases, to determine how many undiagnosed cases can be explained by coding mutations in previously reported disease genes, we detected a relatively low diagnostic yield. MAC phenotypes have a reported sibling risk ratio of 316 to 527, indicating a strong genetic component with both dominant and recessive modes of inheritance observed in families. [30] Previous reports identified a genetic cause for 80% of bilateral anophthalmia and severe microphthalmia cases. [41] Of the 8 individuals with pathogenic variants identified in our study, 6 had bilateral phenotypes and 4 were syndromic. Our study in a cohort comprising more than fifty percent unilateral MAC cases showed that most unilateral microphthalmia and coloboma cases remain unexplained using ACMG criteria and current knowledge of disease genes and Mendelian models of inheritance

Anterior segment dysgenesis including glaucoma Developmental abnormalities of the anterior part of the eye, including the iris and cornea, present highly variable phenotypes ranging from severe to subclinical angle malformation affecting outflow. Individuals with glaucoma and/ or more severe developmental abnormalities of the anterior segment represented the largest sub-group screened.

Of the 113 children, 83 cases (79.6%) had early onset glaucoma (Figure 3D, E). Of these, 23 had ASDA (range of features) as well, while 60 had only glaucoma without obvious anterior segment defects. The remaining 30 children (20.4%) had anterior segment defects without glaucoma at the time of recruitment. Of the 113 children, 14 (12.4%) had extraocular phenotypes (Fig 3 D, E); 13 children had a positive family history, with one or more relatives with a similar phenotype and in 3 cases the parents were consanguineous.

28 of the 113 cases were found to have pathogenic variants in 10 different genes (24.8%). 11 had biallelic (homozygous or compound heterozygous) mutations in *CYP1B1.* Of these, 9 had a diagnosis of primary congenital glaucoma at recruitment and two were described as congenital corneal opacity. 10 cases had dominant mutations in *FOXC1*; of these, two were whole gene deletions and one was a whole gene duplication (structural variant, CNV) (Figure 5). Both cases with *FOXC1* deletion had overt anterior segment dysgenesis (one with secondary glaucoma), whereas the duplication case was recruited with a primary congenital glaucoma diagnosis (with absence of other features). This is in line with the early onset of glaucoma (in first decade; n=18 cases) described in a large pedigree with 6p25 duplication encompassing *FOXC1.* [42] Of the other seven *FOXC1* cases, one individual had been referred with a diagnosis of primary congenital glaucoma (case 152) and two were referred with Axenfeld Rieger syndrome and congenital glaucoma (case 162 &154); the rest were reported anterior segment defects including congenital corneal opacity, and intracorneal cyst.

The remaining pathogenic findings in the childhood glaucoma cases were homozygous mutations, in *LTBP2* and *TREX1.* Overall, this gave a diagnostic yield for childhood glaucoma of 21.7% (18 / 83) and showed a relatively high prevalence of *FOXC1* mutations.

One individual with congenital corneal opacity and irido-corneal adhesions had two heterozygous mutations in two different genes (*MYOC* and *WDR36*), each inherited from a different parent suggesting a clinically composite form of ASDA. [43] Both mutations have previously been reported to cause dominant primary open angle glaucoma (POAG). [44, 45] Dominant pathogenic variants were identified in *COL4A1*, *FOXE3* and *PAX6* in individuals with microcornea, corneal opacity and aniridia respectively, without glaucoma. One of these cases (Case 81), with congenital corneal opacities and iridocorneal adhesions, had a previously reported dominant stop-loss variant in *FOXE3* (Figure 4H), [46] which had a likely gain of function effect. [26] Segregation analysis showed that he inherited it from his father who had microcornea and cataract. The *COL4A1* mutation is also previously reported and causes the syndromic condition brain small vessel disease with ocular anomalies, which can include cataract, microcornea and Axenfeld Rieger phenotypes. [47] In case 236 at the time of recruitment no extra ocular features were reported. Detailed phenotypes for all cases are given in Supplementary Table 2.

Two previously reported pathogenic mutations were found in *VSX1* and *TGFBI,* which did not fit the reported phenotype and are presumed not pathogenic in this study. [48, 49] The variant in *VSX1* was reclassified as a variant of uncertain significance by a subsequent publication. [50]

Syndromic and other phenotypes 7 cases recruited presented diverse ophthalmological and systemic phenotypes that could not be classified into one of the above groups, plus one case with albinism. In two cases with different ocular phenotypes (Case 59 and 60) we identified the same homozygous, premature stop codon in *SRD5A3* a known cause of disorder of glycosylation. [51] Sequencing of the individual with albinism initially identified a single heterozygous pathogenic missense in an albinism gene *OCA2*, although a second structural variant in the same gene was identified later (see below)

Retinal dystrophies The group of early onset retinal dystrophies showed a relatively high diagnostic yield (40%) with 21 molecular diagnoses made out of 49 cases of early onset retinal dystrophy (EORD) screened (Table 2).

CNGA3 accounted for the highest mutational load with pathogenic, biallelic variants identified in 5 cases described as cone dystrophy or achromatopsia. Four other cases, three diagnosed as achromatopsia and one with a severe rod-cone dystrophy (Case 266), had pathogenic biallelic variants in *CNGB3*. Three cases referred with Stargardt's disease had pathogenic biallelic variants in *ABCA4.*

The remaining pathogenic variants identified were in *RDH12*, *CRB1*, *COL2A1*, *GUCY2D*, *RPE65*, *CACNA1F, RAX2, PROM1* and *TSPAN12*. Of the 8 possible compound heterozygous pathogenic variants identified, segregation analysis was carried out for 5 cases and all of these were proved to be compound heterozygous, Figure 5 H, I, J.

The diagnostic yield obtained was comparable to that obtained by other recent retinal dystrophy specific gene panel tests. [16, 52] However, diagnostic yield is likely to vary based on the composition of the patient cohort.

The diagnosis rate for retinal dystrophies was lower in our study compared to several other NGS based studies, which may be due to a number of factors. The retinal cohort was small (49 individuals), whereas other studies have screened larger cohorts, [53-55] as retinal dystrophies are genetically and phenotypically diverse the range of phenotypes covered in our cohort may differ from those reported in other studies. For example, Eisenberger et al, who report a higher diagnostic yield included only individuals with Leber's Congenital Amaurosis or Retinitis Pigmentosa. [54] Also, we screened only childhood cases, of early onset retinal dystrophy, which may not be representative of the range of retinal dystrophy phenotypes present in adult populations. Two individuals had single heterozygous variants in recessive genes. They may have second deep intronic /regulatory variants, which were not investigated in this study.

Congenital cataracts Both autosomal dominant and recessive inheritance is seen in congenital cataracts. [13] Eight cases of the nine congenital cataract cases screened were detected positive for likely dominant pathogenic mutations, giving a diagnostic yield of 88.9%. All except one of the variants detected were novel and heterozygous. The genes harbouring these variants were *CRYAA* (2 cases), *CRYGD* (2 cases), *CRYBA1*, *GJA8*, *MAF* and *EPHA2.* The variant in *EPHA2* was intronic and not located in the canonical splice site but had previously been reported as pathogenic and shown to affect splicing [56] Previous cataract-specific gene panels have reported a diagnostic yield near 75%. [13]

CRYBA1 (Case 187) presented with pseudo-aphakic glaucoma after earlier cataract surgery. One of the *CRYGD* cases (case 290) had microphthalmia and cataracts.

Analysis for larger structural variants

Aligned sequence data from the Oculome panel was also analysed to identify signatures of larger insertions, deletions and inversions across the cohort, using a read depth based algorithm ExomeDepth. We identified likely pathogenic copy number variants, which met with the standards recommended by the ACMG, [57] in four individuals. Plots of observed by expected read depth ratio of the regions with copy number variation in these individuals are shown in Figure 6. Regions with copy number variations show an observed by expected read depth ratio outside the normal range.

Two heterozygous deletions and one heterozygous duplication involving the whole of *FOXC1*, were identified in three individuals with ASDA phenotypes. Loss of function mutations and whole gene deletions, as well as increased dosage of *FOXC1,* have been previously reported to cause anterior segment dysgenesis phenotypes associated with glaucoma. [27, 42, 58]

In the individual with albinism, analysis for coding variants initially identified a previously reported pathogenic missense variant in the gene *OCA2*, in heterozygous form. The CNV analysis pipeline identified a second variant – a heterozygous deletion of exon 7 of *OCA2*, highlighting the benefit of simultaneous analysis for both types of variants. Variants in *OCA2* have previously been associated with only recessively inherited oculocutaneous albinism (OMIM: 203200).

In addition, CNVs with an uncertain clinical significance were identified in 2 cases with MAC phenotype (Fig 3 E, F,G). Case 253, a male, with retinal coloboma, cleft lip and palate, hearing loss and growth hormone deficiency had a hemizygous duplication on chromosome X involving the gene *NDP*. Case 110, with unilateral microphthalmos and strabismus had a large heterozygous deletion on Chromosome 10 involving the genes *ERCC6* and *RBP3,* which are part of the capture panel. Exact break point of the indels could not be mapped from the oculome data.

Ethnicity The largest ethnic group represented in our cohort was White European (139), Followed by South Asian ethnicities (21, including Indian, Pakistani and Bangladeshi ethnicities), followed by Black-African (7), Arabic / Middle Eastern (5) and Black Caribbean (2). For a large number of individuals (91), the ethnicity was unknown, and an additional 12 individuals were of mixed ethnicity or ethnicities that could not be classified into one of the above groups. While the numbers were too low to calculate diagnostic yields separately for each phenotype and ethnic group, the two largest ethnic groups, White European and South Asian, had overall diagnostic yields of 20.14% and 52.38% respectively. Of the 28 White European individuals with pathogenic variants, 11 had dominant variants, 10 recessive compound heterozygous, 6 homozygous and one had an X-linked variant. Of the 11 South Asian individuals with pathogenic variants, 2 had dominant variants, 2 recessive compound heterozygous, 7 recessive homozygous and one had an X-linked variant.

Variants of uncertain significance in relevant genes

Supplementary Table 3 details MAC and ASDA cases with rare or novel missense variants of uncertain significance (VUS; Class 3) in relevant genes. These were the two phenotypic groups with the lowest diagnostic yields (class 4 or 5 variants). The majority of Class 3 variants were missense variants. They were further annotated using the in-silico prediction programs SIFT, Polyphen, Mutation Taster and FATHMM and CADD scores. [59] CADD scores were developed as a measure of deleteriousness, incorporating multiple annotations; deleterious variants have higher CADD scores. Of the 64 Class 3 variants, 6 had CADD scores above 30, identifying them as most likely to be deleterious. An additional 33 variants had CADD scores between 20 and 30. Reporting variants of unknown significance in a broad range of eye disease genes may over time provide a richer understanding of variation in the presentation of disease phenotypes in individuals.

Discussion

In this study we demonstrate that it is possible to simultaneously screen a comprehensive panel of genes affecting the development of the eye. The Oculome multi-gene panel test provides a convenient and cost-effective route for diagnostic genetic testing, and includes exome gene sub panels for childhood glaucoma and MAC, which have not previously been evaluated as diagnostic test panels. Multi-gene panel assays enable clinicians to provide a targeted diagnosis to families and to initiate appropriate management, not only for the eye condition, but for any potential systemic conditions. We showed that the Oculome test identified pathogenic variants in a cohort of children presenting with developmental eye conditions. We determined the proportion of cases that can be explained by coding mutations in currently known disease genes, and compared diagnosis between phenotypic groups. Several novel pathogenic variants were identified contributing to knowledge of genotype phenotype correlations; of a total of 98 pathogenic variants

42 (42.8%) were novel pathogenic variants. The rest had previously been reported as pathogenic/likely pathogenic in Clinvar/dbSNP/OMIM.

The diagnostic yield varied considerably with the type of condition, being higher for retinal dystrophies and congenital cataracts (40.3 to 88.9%) and lower for MAC and ASDA (8.2 to 23.7%) indicating the current state of knowledge of the aetiology underlying these conditions. For MAC, diagnosis was achieved primarily for syndromic and bilateral cases. To our knowledge, few studies have previously screened large or diverse groups of children with MAC or ASDA phenotypes. These diagnostic yields indicate that future genome wide analysis offers potential for discovery of novel genes underlying MAC and ASD phenotypes. The diagnostic yields for retinal dystrophies and congenital cataracts were comparable to yields achieved by previous disease-specific gene panels. [13, 16, 52]

Limitations

Our study of a population of children presenting mainly at two centres in the UK, induces some selection bias. However, as our population is ethnically diverse and geographically draws on communities across the UK and Europe, it is likely that the diagnostic yield will be similar in other settings. In our study cohort, we detected pathogenic variants in 68 cases.

5’ UTRs and introns were not included in our capture design as there is not yet an established method for predicting the functional effect of novel intronic or 5’ UTR variants. However, probes for selected, known intronic variants of proven pathogenicity could be included in future iterations of the panel. For example, a deep intronic variant in *CEP290* is known to account for a large proportion of cases with Leber’s Congenital Amaurosis. [60] Our cohort included at least three individuals with heterozygous known pathogenic variants in a relevant gene but with no second mutation in the same gene (1 variant each in *IQCB1*, *CNGB3* and *CYP1B1*); future research into intronic and long range gene regulatory sequences may identify relevant sequences. The gene *RBP4* has been shown to have a dominant inheritance pattern, with incomplete penetrance, but increased severity if the variant is inherited from the mother. [61] In our study we discounted variants that did not segregate so would miss the significance of variants with variable penetrance.

The robust methodology we employed allowed us over the two iterations of the Oculome gene panel to demonstrate significant improvement in depth of coverage from 95% to 99.5% sequenced at greater than 30X depth (see Supplementary Figure 1). Our design paid special attention to the gene *FOXC1* adding additional cRNA baits in an attempt to boost capture. We successfully identified the positive control mutations in *FOXC1* as well as an additional 7 pathogenic SNVs or small Indels and 3 CNVs, whereas previous panels have failed to detect mutations in *FOXC1.* [62] The final coverage achieved by the Oculome panel is comparable to, or better, than that achieved by several disease-specific eye gene panels. [13, 52, 62] Previous studies have reported that panel tests are more sensitive than whole exomes in detecting variants [62] and they are currently cheaper for diagnostic testing. [63] Based on more recent studies, this difference in sensitivity between gene panels and exome sequencing has been decreasing. [64] If costs of next generation sequencing also decrease considerably, whole genome sequencing with analysis of phenotype-specific virtual gene panels will become an attractive alternative. This approach would allow the constant expansion of panels with newly discovered disease genes. As whole genome sequencing omits the capture step during library preparation, it is reported to achieve better coverage of exonic regions than exome sequencing. [65]

Benefits of using large and diverse gene panels demonstrated by several cases in our cohort

Reaching a molecular diagnosis in childhood ocular conditions is hampered by the large number of genes involved, as well as overlapping, complex or ambiguous phenotypes. These difficulties lead to a higher likelihood of incorrect clinical diagnosis. Providing a genetic diagnosis can help refine the initial diagnosis. This can mean more appropriate disease management and a different disease course or prognosis (e.g. stationary or progressive). Genetic diagnosis can assist the family in planning future pregnancies and may assist in predictive counselling. The very large number of genes implicated in many of the phenotypes means that the most efficient possibility for arriving at a genetic diagnosis is to use large multi-gene panels. Simultaneous screening of many disease genes may also help identify unusual and new associations between genes and phenotypes that would not have been identified in sequential single gene testing. At a practical level a large panel that combines several phenotypes allows higher throughput of patients by using the same capture probes set for all patients.

For example, Case 223, was referred with congenital glaucoma, cupped optic nerves, cerebral palsy and microcephaly. We identified a homozygous frameshift variant p.Ala221Glyfs*2 in *TREX1*, consistent with a diagnosis of Aicardi-Goutières Syndrome, a severe and progressive condition which was not apparent from the initial clinical examination.

In the case of childhood glaucoma, we found a positive mutation in the most common gene to cause primary congenital glaucoma (*CYP1B1*) in 13.3 % (11 of 83) cases. Of the glaucoma cases negative for this gene, five had a mutation in *FOXC1*, one in *LTBP2* and one in *TREX1* mutation. This means that the Oculome identified a molecular diagnosis in 21.7 % of children with glaucoma and a further 8% were genetically diagnosed as being at risk of developing glaucoma (6 *FOXC1* cases and a composite *MYOC/WDR36* case). Genetic diagnosis may contribute to parents' planning for the future: whilst recessive *CYP1B1* mutations will carry a risk of 25% of future children being affected, *de novo FOXC1* mutations have a low risk of occurring in future offspring. In addition, the affected children themselves may benefit by timely referral for those with *FOXC1* mutations to other specialists to screen and monitor for associated life-threatening cardiovascular defects. [66, 67] There is also a growing body of evidence indicating that the severity of early-onset glaucoma differs between different genetic causes. [25]

Case 74 was referred with an anterior segment dysgenesis phenotype of congenital corneal opacity, iridocorneal adhesions and scleralization of the peripheral cornea. They were found to carry two previously reported pathogenic variants: p.Gln386* in *MYOC*, a risk variant for *POAG,* [45, 68] and p.Asn355Ser in *WDR36*, also causing POAG [44]. However, the phenotype of the patient here is more severe than that reported for either variant alone. The two variants were inherited from different parents and both parents were unaffected.

Case 266 and case 279, in the retinal cohort, were both found to have the same previous reported pathogenic variant, p.Thr383Ilefs*13, in *CNGB3* but have different phenotypes (Figure 5 D, D', E, E'). Case 279 had a phenotype of achromatopsia, while case 266 had a much more severe and progressive retinal dystrophy phenotype with ERGs indicating that both rod and cone photoreceptors were affected. This variant was first identified in a large number of patients with achromatopsia. However, recent studies have shown that a subset of patients with this variant may develop a more severe phenotype [69] consistent with the findings in Case 266. Case 325 had macular dystrophy and a previously reported pathogenic variant p.Arg373C in *PROM1*. This variant had previously been reported in three families with three varying phenotypes; Stargardt-like macular dystrophy, bull's eye macular dystrophy and cone-rod dystrophy. [70]

Case 269 was reported as rod-cone dystrophy, and his brother was similarly affected. His maternal uncle had congenital nystagmus and his maternal grandfather was affected with macular degeneration (Figure 5 I). He was found to have a composite mutation: a Class 4 novel hemizygous nonsense variant p.Arg50*8 in *CACNA1F* and a Class 4 novel heterozygous frameshift variant p.Leu114Alafs*18 in *RAX2*. Hemizygous loss-of-function variants in *CACNA1F* are implicated in Incomplete Congenital Stationary Night Blindness and cone rod dystrophy, with an X linked mode of inheritance, which matches the family history of this case. [71, 72] Electrodiagnostic testing showed a well preserved a-wave and residual rod driven-b wave in keeping with incomplete CSNB with atypically worse cone function. The variant in *RAX2* is at the same position as another frameshift variant reported in a family with dominant slowly progressing cone-rod dystrophy and abnormal electroretinograms. [73] While not consistent with the X-linked recessive mode of inheritance suggested by the family history, it may modify the phenotype.

Similarly, cases 59 and 60 had the same homozygous, previously reported pathogenic, recessive variant in *SRD3A5*, a gene implicated in congenital disorders of glycosylation. This variant has been reported in 4 unrelated families with a congenital disorder of glycosylation with ophthalmologic abnormalities. [51, 74, 75] As in previous reports of this variant, [51] the two cases in our study show different ocular phenotypes. Case 59 was diagnosed with nystagmus, optic nerve hypoplasia and developmental delay. Case 60 was diagnosed with retinal dystrophy and microcephaly.

Analysis of copy number variants

Analysing NGS data for CNVs complements analysis for SNVs and small indels and involves no extra cost. The method of CNV analysis we used is a read depth based approach and therefore does not detect inversions or identify precise breakpoints. [19] Identification of breakpoints is also difficult in a targeted capture panel. However, the CNV analysis acts as a useful tool for prompting follow-up by microarray analysis. Alternatively, an analysis method based on split reads could be used on our sequence data to detect inversion breakpoints, provided that they lie within our target region. [76] We were able to achieve genetic diagnoses in 4 additional cases using CNV analysis. One of these, case 251 (albinism) had a single heterozygous pathogenic missense variant in *OCA2*, a gene implicated in recessively inherited albinism, but lacked a second variant. CNV analysis identified a rare deletion of a different exon of *OCA2*. A large number of patients had CNV calls in the Opsin1LW/MW genes. [77] However, because these genes are very similar in sequence and the number of copies is known to vary, it was difficult to identify disease-causing variant calls.

All the genes investigated in the Oculome panel test have been reported as disease genes in monogenic developmental and inherited eye diseases. However, there is increasing evidence that low penetrance variants in these disease genes may also cause milder phenotypes, or increase the risk of later onset disease. For example, SNPs in *PRSS56* have been associated with myopia involving increased axial length of the eye globe, [78, 79] while homozygous high impact variants cause severe nanophthalmos. [38] Recent genome wide association studies have identified an intronic risk variant in *LMX1B* associated with increased intraocular pressure and primary open angle glaucoma, [80] while high impact exonic variants are known to cause nail patella syndrome and increased risk of glaucoma. [81] Similarly, a risk variant close to *FOXC1* is associated with primary open angle glaucoma, [82] while high impact exonic variants cause anterior segment anomalies. [58] It is also possible that some of the individuals in the Oculome cohort have severe, but polygenic, phenotypes. The analysis pipeline for the Oculome panel was designed to detect monogenic pathogenic variants with complete penetrance. However, a number of Class 3 variants were also identified, including variants in *FOXC1* and *LMX1B*. In several cases segregation analysis in the parents of the proband did not produce evidence supporting pathogenicity (Supplementary Table 3). While none of the class

3 variants had enough evidence to show that they were individually pathogenic, some may be low penetrance variants and/or contribute to a polygenic form of the phenotype.

Conclusions

In conclusion, the Oculome NGS assay can provide a molecular diagnosis to families of children with developmental eye defects beyond the range of conditions included in comparable panel assays. Understanding the genetic cause allows the clinician to arrange appropriate genetic counselling, which may include testing other family members for carrier status or prenatal screening, provide a prognostic outlook, and arrange novel treatments such as gene or cell therapies as these become available. Where no treatment is available, a molecular diagnosis and prognosis may allow the family to prepare and plan for the future and to access the support their child requires.

ACKNOWLEDGEMENTS

This article is dedicated to our late colleague, co-author and friend, Prof Maria Bitner-Glindzicz.

We are very grateful to all colleagues in the Clinical and Academic Department of Ophthalmology, Clinical Genetics and the North East Thames Laboratory at GOSH and at GOSICH, Moorfields Eye Hospital and at Medical Genetics, Genova who contributed to this study. This work was generously supported by the Rosetrees Trust, Moorfields Eye Hospital Special Trustees, Microphthalmia, Anophthalmia and Coloboma Support (MACS), Action Medical Research, the National Institute for Health Research (NIHR) Great Ormond Street Hospital Biomedical Research Centre, and the NIHR Moorfields Biomedical Research Centre. J.C.S. is funded by the Great Ormond Street Hospital Children’s Charity and is an NIHR Senior Investigator. A. P. is a recipient of a UCL Graduate Research Scholarship and UCL Overseas Research Scholarship. L.E.V is funded by a FONDECYT grant (11160951). The views expressed are those of the authors and not necessarily those of the NHS, the NIHR or the Department of Health. Our particular thanks go to the children who took part in this study and their families, who selflessly gave their time to help other children in the future.

List of Figures

Figure 1 Study cohort and gene panel

A. Venn diagram depicting the 429 genes arranged on the Oculome as virtual gene panels for each phenotypic subgroup: shows the number of genes that cause phenotypes in more than one phenotypic sub group. ASDA, anterior segment developmental anomalies including glaucoma; MAC, disorders of the globe; RET, retinal dystrophies; CAT, cataracts and lens associated conditions; SYN/O, syndromic conditions not fitting into other sub groups.

B. Pie chart representing phenotypic sub groups of 277 participating children.

Figure 2. Variant classification pipeline.

Variants were interpreted in accordance with ACMG guidelines [18]. Class 4 and class 5 are predicted pathogenic variants as they are either known published mutations, or loss of function (splice site, frameshift, or nonsense) variants, or predicted damaging missense variants with additional evidence. Class 3 (VUS) are missense variants in a relevant gene without functional or segregation studies or other evidence to prove pathogenic consequence. Class 2 included variants previously reported as benign / likely benign, variants present in multiple individuals in the run, variants that do not match the inheritance pattern of the gene (e.g. single heterozygous variant for recessive condition), and intronic variants that lie outside of canonical splice sites. Class 1 variants are filtered out at the first stage (variants >2% in ExAC, EVS or 1000 Genomes). Variants are interpreted according to phenotype (OMIM), mode of inheritance for condition, mutation impact, in-silico prediction tools, database search (dbSNP, DECIPHER), functional domain, evolutionary conservation, published functional studies and segregation within family. Following these analyses variants may be re-classified. MAF = Minor Allele Frequency; EVS= Exome Variant Server.

Figure 3: Characteristics of MAC and ASDA phenotypic groups.

A-C Pie charts showing the proportion of individuals with Microphthalmia, Anophthalmia and/or Coloboma (MAC) (n = 98), with and without optic fissure closure defects (A) or extraocular phenotypes (Syndromic MAC) (B) and unilateral or bilateral phenotypes. (C)

D, E Pie charts showing the proportion of individuals with Anterior Segment Developmental Anomalies (ASDA) (n= 113) with childhood glaucoma and anomalies apparent in the anterior segment, congenital glaucoma alone, and anterior segment anomalies without glaucoma (D), and individuals with extraocular phenotypes (syndromic) (E).

Figure 4: Phenotype images and results of segregation analysis (MAC and ASDA).

A-F Segregation of the variant with disease phenotype in families with MAC (Cases 25, 112, 12, 190, 260, 10). E' Macular and OCT images of the retina in Case 260 showing macular folds. F': Microphthalmic eye in Case 294. G: De-novo variant in *FOXC1* in Case 10 with MAC and anterior segment dysgenesis. H: Co-segregation of a variant in *FOXE3* with disease phenotype in a family (proband case 81) with anterior segment dysgenesis. Black: affected, White: unaffected, ?: Genotype/phenotype unknown. CCO, congenital corneal opacity; ICA, irido-corneal adhesions.

Figure 5: Phenotype images and results of segregation analysis (Retinal dystrophies).

A-C: Segregation of known/likely (class 4/5) pathogenic variants in *CNGA3* in individuals with achromatopsia. D,E: Segregation of a known pathogenic frameshift variant in CNGB3 in one individual with severe rod-cone dystrophy and another individual with the milder phenotype of achromatopsia. D', E': Fundus autoflorescence imaging of the two probands in D and E demonstrating hyper-autofluresecence at the fovea. F,G: Segregation of known/likely pathogenic variants in *ABCA4* in individuals with Stargardt's disease. G': Widefield retinal image of the proband in pedigree G. Segregation of a likely pathogenic variant in RPE65 with the phenotype in an individual with cone-rod dystrophy. The proband also carries a variant in *PDE6B* that does not segregate with the phenotype. I: Variants in *CACNA1F* and *RAX2* in an individual with achromatopsia. J: Segregation of a likely pathogenic variant in *COL2A1* with the phenotype in a father and daughter with Stickler syndrome.

Figure 6: Copy Number Variant Calls.

A: A heterozygous deletion of exon 7 of *OCA2* in an individual with oculocutaneous albinism. B: a heterozygous duplication of *FOXC1* in an individual with an ASD phenotype. C, D: heterozygous deletions of *FOXC1* in individuals with ASD phenotypes. E-G: CNV variants of uncertain significance in individuals with MAC phenotypes. The Y axis shows the ratio of observed reads by expected reads observed for each exon of the gene of interest. Red dotted lines mark thresholds determining significant copy number changes. Chromosomal location according the reference human genome Hg19. Only coding exons, which were targeted in the Oculome capture are shown. CNV plots generated were using Exome Depth tool.

List of Tables

Table 1. Data output for each rapid sequencing run.

Run information for high-throughput sequencing runs in study performed on the Illumina MiSeq (Pilot Oculome 1) or Illumina HiSeq2500 using a rapid run mode flow cell. Oculome v2.1 to 2.3 showed improved coverage and mean read depth compared to early runs. PF = passing filter.

Table 2 Table 2. Diagnostic yield (Clinical class 4/5) varied between 8.2% and 88.9% depending on the phenotype

Table 3. Likely pathogenic or known pathogenic variants (Clinical class 4 or 5). All class 4 or 5 variant detected in the study subdivided by phenotypic sub-panel (Pink: MAC, Green: ASDA, Yellow: Retinal Dystrophies, Blue: Congenital cataracts,

Grey: Oculocutaneous albinism and others). Clinical diagnosis following mutation analysis is given in column 'Genetic Diagnosis'. 61 diagnoses were made out of 254 cases analysed. 25 had dominant variants and 35 had recessive variants (homozygous or compound heterozygous), and 1 case composite. Minor allele frequencies (MAF) were extracted from ExAc (http://exac.broadinstitute.org/), which includes genetic variation derived from 60,706 unrelated individuals. Exact breakpoints ofr structural variants could not be mapped. The extent of structural variants shown in this table indicate the overlap of the structural variant with our target region. [a] This variant was inherited from the apparently asymptomatic mother but may modify the phenotype. [b] This variant is outside the splice site but is a previously reported pathogenic variant.

Supplementary information

Supplementary Table 1: Full gene list and overlapping gene panel lists on the oculome

Supplementary Table 2: Details of phenotypes of individuals with class 4/5 genetic diagnoses from the oculome NR: Not reported W: White, A(I): Asian / Asian British - Indian, A(P): Asian / Asian British - Pakistani, A(B): Asian / Asian British - Bangladeshi, A(C): Asian / Asian British Chinese, A(O): Asian / Asian British Other, B(A): Black / Black British –African, B(C): Black / Black British –Carribean, Ar: Arab. If visual acuity was recorded as "counting fingers", a BCVA of 2.1 logMAR was noted, for "hand movements only" 2.4 logMAR, for "perception of light" 2.7 logMAR, and for "no perception of light" or "ocular prosthesis/artificial eye", 3 logMAR.

Supplementary Table 3: Variants of uncertain significance (Class 3) in cases. The first column indicates the case number and phenotype in brief (MAC cohort: highlighted pink, ASDA/Glaucoma cohort: highlighted green). Where a variant is located in a known protein domain, this has been indicated. Orange boxes indicate variants that did not segregate with the phenotype. Yellow boxes indicate cases identified with single heterozygous variants in relevant recessive genes, but lacking second variants. The final column lists the ExAC constraint metric for the gene (http:unkexac.broadinstitute.org/); z-scores indicate tolerance to missenses, with higher values meaning decreased tolerance and pLI indicates tolerance to loss of function mutation (pLI >= 0.9 genes are very tolerant to loss of function).*Case 11: Variant previously reported pathogenic along with a variant in GDF3. In case 11 there was no variant in GDF3 and variant in GDF6 did not segregate. Congenital glaucoma cases 30 & 35 have variants in the COL4A1 gene; small vessel disease of the brain with ocular anomalies including glaucoma and anterior segment anomalies (Axenfeld Rieger) can be caused by heterozygous COL4A1 mutation. C: coloboma, M: microphthalmia, ASDA: anterior segment developmental anomalies, GLAU: childhood glaucoma, CD: Corneal Dystrophy N-S: reported as non-syndromic, ND: not done, NA: not available, S: SIFT (sift.bii.a-star.edu.sg/), P: PolyPhen (genetics.bwh.harvard.edu/pph2/), MT: Mutation Taster (www.mutationtaster.org/), F: FATHMM (fathmm.biocompute.org.uk/). T: Tolerated, D: Deleterious, B: Benign, PosD: Possibly Damaging, ProD: Probably Damaging, Pol: Polymorphism, DC: Disease Causing.

Supplementary Figure 1. Coverage graphs indicating increased coverage over the two iterations of the Oculome capture panel.

A: Mean depth of coverage across 88 samples screened with Oculome version 1. B: Percentage of the target covered with a read depth of at least 30X in the 88 samples run on Oculome v1. C: Mean depth of coverage across 64 samples screened on Oculome v2.1. The samples showed higher mean depth of coverage. D: Percentage of the target covered with a read depth of at least 30X in the first 64 samples run on Oculome v2.1.

References

1. Gilbert, C. and A. Foster, Childhood blindness in the context of VISION 2020--the right to sight. *Bull World Health Organ*, 2001. **79**(3): 227-32.
2. Kong, L., et al., An update on progress and the changing epidemiology of causes of childhood blindness worldwide. *J AAPOS*, 2012. **16**(6): 501-7.
3. Shah, S.P., et al., Anophthalmos, microphthalmos, and typical coloboma in the United Kingdom: a prospective study of incidence and risk. *Invest Ophthalmol Vis Sci*, 2011. **52**(1): 558-64.

4. Papadopoulos, M., et al., The British Infantile and Childhood Glaucoma (BIG) Eye Study. *Invest Ophthalmol Vis Sci*, 2007. **48**(9): 4100-6.
5. Rahi, J.S., C. Dezateux, and G. British Congenital Cataract Interest, Measuring and interpreting the incidence of congenital ocular anomalies: lessons from a national study of congenital cataract in the UK. *Invest Ophthalmol Vis Sci*, 2001. **42**(7): 1444-8.
6. Hamblion, E.L., et al., Incidence and patterns of detection and management of childhood-onset hereditary retinal disorders in the UK. *Br J Ophthalmol*, 2012. **96**(3): 360-5.
7. Hartong, D.T., E.L. Berson, and T.P. Dryja, Retinitis pigmentosa. *Lancet*, 2006. **368**(9549): 1795-809.
8. Khordadpoor-Deilamani, F., et al., Sequence analysis of tyrosinase gene in ocular and oculocutaneous albinism patients: introducing three novel mutations. *Mol Vis*, 2015. **21**: 730-5.
9. Raca, G., et al., Next generation sequencing in research and diagnostics of ocular birth defects. *Mol Genet Metab*, 2010. **100**(2): 184-92.
10. Thusberg, J., A. Olatubosun, and M. Vihinen, Performance of mutation pathogenicity prediction methods on missense variants. *Hum Mutat*, 2011. **32**(4): 358-68.
11. Neveling, K., et al., Next-generation genetic testing for retinitis pigmentosa. *Hum Mutat*, 2012. **33**(6): 963-72.
12. Jiang, Q., et al., Rapid and efficient human mutation detection using a bench-top next-generation DNA sequencer. *Hum Mutat*, 2012. **33**(1): 281-9.
13. Gillespie, R.L., et al., Personalized diagnosis and management of congenital cataract by next-generation sequencing. *Ophthalmology*, 2014. **121**(11): 2124-37 e1-2.
14. Gillespie, R.L., et al., Next-generation Sequencing in the Diagnosis of Metabolic Disease Marked by Pediatric Cataract. *Ophthalmology*, 2016. **123**(1): 217-20.
15. Musleh, M., et al., Diagnosing the cause of bilateral paediatric cataracts: comparison of standard testing with a next-generation sequencing approach. *Eye (Lond)*, 2016. **30**(9): 1175-81.
16. Ellingford, J.M., et al., Molecular findings from 537 individuals with inherited retinal disease. *J Med Genet*, 2016.
17. Day, A.C., et al., The Royal College of Ophthalmologists' National Ophthalmology Database study of cataract surgery: report 1, visual outcomes and complications. *Eye (Lond)*, 2015. **29**(4): 552-60.
18. Richards, S., et al., Standards and guidelines for the interpretation of sequence variants: a joint consensus recommendation of the American College of Medical Genetics and Genomics and the Association for Molecular Pathology. *Genet Med*, 2015. **17**(5): 405-24.
19. Plagnol, V., et al., A robust model for read count data in exome sequencing experiments and implications for copy number variant calling. *Bioinformatics*, 2012. **28**(21): 2747-54.
20. Conrad, D.F., et al., Origins and functional impact of copy number variation in the human genome. *Nature*, 2010. **464**(7289): 704-12.
21. Gould, D.B. and S.W. John, Anterior segment dysgenesis and the developmental glaucomas are complex traits. *Hum Mol Genet*, 2002. **11**(10): 1185-93.
22. Ito, Y.A. and M.A. Walter, Genomics and anterior segment dysgenesis: a review. *Clin Exp Ophthalmol*, 2014. **42**(1): 13-24.
23. Lewis, C.J., et al., Primary congenital and developmental glaucomas. *Hum Mol Genet*, 2017. **26**(R1): R28-R36.
24. Berger, W., B. Kloeckener-Gruissem, and J. Neidhardt, The molecular basis of human retinal and vitreoretinal diseases. *Prog Retin Eye Res*, 2010. **29**(5): 335-75.
25. Kelberman, D., et al., Digenic inheritance of mutations in FOXC1 and PITX2 : correlating transcription factor function and Axenfeld-Rieger disease severity. *Hum Mutat*, 2011. **32**(10): 1144-52.

26. Islam, L., et al., Functional analysis of FOXE3 mutations causing dominant and recessive ocular anterior segment disease. *Hum Mutat*, 2015. **36**(3): 296-300.
27. Lehmann, O.J., et al., Ocular developmental abnormalities and glaucoma associated with interstitial 6p25 duplications and deletions. *Invest Ophthalmol Vis Sci*, 2002. **43**(6): 1843-9.
28. Bardakjian, T., et al., A recurrent, non-penetrant sequence variant, p.Arg266Cys in Growth/Differentiation Factor 3 (GDF3) in a female with unilateral anophthalmia and skeletal anomalies. *Am J Ophthalmol Case Rep*, 2017. **7**: 102-106.
29. Ye, M., et al., Mutation of the bone morphogenetic protein GDF3 causes ocular and skeletal anomalies. *Hum Mol Genet*, 2010. **19**(2): 287-98.
30. Morrison, D., et al., National study of microphthalmia, anophthalmia, and coloboma (MAC) in Scotland: investigation of genetic aetiology. *J Med Genet*, 2002. **39**(1): 16-22.
31. Shah, S.P., et al., Anophthalmos, microphthalmos, and Coloboma in the United kingdom: clinical features, results of investigations, and early management. *Ophthalmology*, 2012. **119**(2): 362-8.
32. Fares-Taie, L., et al., ALDH1A3 mutations cause recessive anophthalmia and microphthalmia. *Am J Hum Genet*, 2013. **92**(2): 265-70.
33. Casey, J., et al., First implication of STRA6 mutations in isolated anophthalmia, microphthalmia, and coloboma: a new dimension to the STRA6 phenotype. *Hum Mutat*, 2011. **32**(12): 1417-26.
34. Segel, R., et al., Pulmonary hypoplasia-diaphragmatic hernia-anophthalmia-cardiac defect (PDAC) syndrome due to STRA6 mutations--what are the minimal criteria? *Am J Med Genet A*, 2009. **149A**(11): 2457-63.
35. Rainger, J., et al., Loss of the BMP antagonist, SMOC-1, causes Ophthalmo-acromelic (Waardenburg Anophthalmia) syndrome in humans and mice. *PLoS Genet*, 2011. **7**(7): e1002114.
36. Okada, I., et al., SMOC1 is essential for ocular and limb development in humans and mice. *Am J Hum Genet*, 2011. **88**(1): 30-41.
37. Asai-Coakwell, M., et al., GDF6, a novel locus for a spectrum of ocular developmental anomalies. *Am J Hum Genet*, 2007. **80**(2): 306-15.
38. Gal, A., et al., Autosomal-recessive posterior microphthalmos is caused by mutations in PRSS56, a gene encoding a trypsin-like serine protease. *Am J Hum Genet*, 2011. **88**(3): 382-90.
39. Wang, X., et al., Mutations in X-linked PORCN, a putative regulator of Wnt signaling, cause focal dermal hypoplasia. *Nat Genet*, 2007. **39**(7): 836-8.
40. Fetterman, C.D., F. Mirzayans, and M.A. Walter, Characterization of a novel FOXC1 mutation, P297S, identified in two individuals with anterior segment dysgenesis. *Clin Genet*, 2009. **76**(3): 296-9.
41. Williamson, K.A. and D.R. FitzPatrick, The genetic architecture of microphthalmia, anophthalmia and coloboma. *European Journal of Medical Genetics*, 2014.
42. Lehmann, O.J., et al., Chromosomal duplication involving the forkhead transcription factor gene FOXC1 causes iris hypoplasia and glaucoma. *Am J Hum Genet*, 2000. **67**(5): 1129-35.
43. Wright, C.F., et al., Genetic diagnosis of developmental disorders in the DDD study: a scalable analysis of genome-wide research data. *Lancet*, 2015. **385**(9975): 1305-14.
44. Monemi, S., et al., Identification of a novel adult-onset primary open-angle glaucoma (POAG) gene on 5q22.1. *Hum Mol Genet*, 2005. **14**(6): 725-33.
45. Stone, E.M., et al., Identification of a gene that causes primary open angle glaucoma. *Science*, 1997. **275**(5300): 668-70.
46. Iseri, S.U., et al., Seeing clearly: the dominant and recessive nature of FOXE3 in eye developmental anomalies. *Hum Mutat*, 2009. **30**(10): 1378-86.
47. Shah, S., et al., Childhood presentation of COL4A1 mutations. *Dev Med Child Neurol*, 2012. **54**(6): 569-74.

48. Boutboul, S., et al., A subset of patients with epithelial basement membrane corneal dystrophy have mutations in TGFBI/BIGH3. *Hum Mutat*, 2006. **27**(6): 553-7.

49. Heon, E., et al., VSX1: a gene for posterior polymorphous dystrophy and keratoconus. *Hum Mol Genet*, 2002. **11**(9): 1029-36.

50. Dash, D.P., et al., Mutational screening of VSX1 in keratoconus patients from the European population. *Eye (Lond)*, 2010. **24**(6): 1085-92.

51. Morava, E., et al., A novel cerebello-ocular syndrome with abnormal glycosylation due to abnormalities in dolichol metabolism. *Brain*, 2010. **133**(11): 3210-20.

52. Carrigan, M., et al., Panel-Based Population Next-Generation Sequencing for Inherited Retinal Degenerations. *Sci Rep*, 2016. **6**: 33248.

53. Weisschuh, N., et al., Mutation Detection in Patients with Retinal Dystrophies Using Targeted Next Generation Sequencing. *PLoS One*, 2016. **11**(1): e0145951.

54. Eisenberger, T., et al., Increasing the yield in targeted next-generation sequencing by implicating CNV analysis, non-coding exons and the overall variant load: the example of retinal dystrophies. *PLoS One*, 2013. **8**(11): e78496.

55. Dockery, A., et al., Target 5000: Target Capture Sequencing for Inherited Retinal Degenerations. *Genes (Basel)*, 2017. **8**(11).

56. Zhang, T., et al., Mutations of the EPHA2 receptor tyrosine kinase gene cause autosomal dominant congenital cataract. *Hum Mutat*, 2009. **30**(5): E603-11.

57. Kearney, H.M., et al., American College of Medical Genetics standards and guidelines for interpretation and reporting of postnatal constitutional copy number variants. *Genet Med*, 2011. **13**(7): 680-5.

58. Nishimura, D.Y., et al., A spectrum of FOXC1 mutations suggests gene dosage as a mechanism for developmental defects of the anterior chamber of the eye. *Am J Hum Genet*, 2001. **68**(2): 364-72.

59. Kircher, M., et al., A general framework for estimating the relative pathogenicity of human genetic variants. *Nat Genet*, 2014. **46**(3): 310-5.

60. den Hollander, A.I., et al., Mutations in the CEP290 (NPHP6) gene are a frequent cause of Leber congenital amaurosis. *Am J Hum Genet*, 2006. **79**(3): 556-61.

61. Chou, C.M., et al., Biochemical Basis for Dominant Inheritance, Variable Penetrance, and Maternal Effects in RBP4 Congenital Eye Disease. *Cell*, 2015. **161**(3): 634-646.

62. Consugar, M.B., et al., Panel-based genetic diagnostic testing for inherited eye diseases is highly accurate and reproducible, and more sensitive for variant detection, than exome sequencing. *Genet Med*, 2015. **17**(4): 253-61.

63. van Nimwegen, K., et al., A Next-Generation Framework: Deciding On The Role Of Costs In The Clinical Use Of Targeted Gene Panels, Exome And Genome Sequencing. *Value Health*, 2015. **18**(7): A352.

64. LaDuca, H., et al., Exome sequencing covers >98% of mutations identified on targeted next generation sequencing panels. *PLoS One*, 2017. **12**(2): e0170843.

65. Meienberg, J., et al., Clinical sequencing: is WGS the better WES? *Hum Genet*, 2016. **135**(3): 359-62.

66. Gripp, K.W., et al., Cardiac anomalies in Axenfeld-Rieger syndrome due to a novel FOXC1 mutation. *Am J Med Genet A*, 2013. **161A**(1): 114-9.

67. Ovaert, C., et al., FOXC1 haploinsufficiency due to 6p25 deletion in a patient with rapidly progressing aortic valve disease. *Am J Med Genet A*, 2017. **173**(9): 2489-2493.

68. Craig, J.E., et al., Evidence for genetic heterogeneity within eight glaucoma families, with the GLC1A Gln368STOP mutation being an important phenotypic modifier. *Ophthalmology*, 2001. **108**(9): 1607-20.

69. Maguire, J., et al., CNGB3 mutations cause severe rod dysfunction. *Ophthalmic Genet*, 2017: 1-7.

70. Yang, Z., et al., Mutant prominin 1 found in patients with macular degeneration disrupts photoreceptor disk morphogenesis in mice. *J Clin Invest*, 2008. **118**(8): 2908-16.

71. Bech-Hansen, N.T., et al., Loss-of-function mutations in a calcium-channel alpha1-subunit gene in Xp11.23 cause incomplete X-linked congenital stationary night blindness. *Nat Genet*, 1998. **19**(3): 264-7.

72. Jalkanen, R., et al., X linked cone-rod dystrophy, CORDX3, is caused by a mutation in the CACNA1F gene. *J Med Genet*, 2006. **43**(8): 699-704.

73. Yang, P., et al., Autosomal Dominant Retinal Dystrophy With Electronegative Waveform Associated With a Novel RAX2 Mutation. *JAMA Ophthalmol*, 2015. **133**(6): 653-61.

74. Cantagrel, V., et al., SRD5A3 is required for converting polyprenol to dolichol and is mutated in a congenital glycosylation disorder. *Cell*, 2010. **142**(2): 203-17.

75. Kara, B., et al., Adult phenotype and further phenotypic variability in SRD5A3-CDG. *BMC Med Genet*, 2014. **15**: 10.

76. Layer, R.M., et al., LUMPY: a probabilistic framework for structural variant discovery. *Genome Biol*, 2014. **15**(6): R84.

77. Nathans, J., D. Thomas, and D.S. Hogness, Molecular genetics of human color vision: the genes encoding blue, green, and red pigments. *Science*, 1986. **232**(4747): 193-202.

78. Kiefer, A.K., et al., Genome-wide analysis points to roles for extracellular matrix remodeling, the visual cycle, and neuronal development in myopia. *PLoS Genet*, 2013. **9**(2): e1003299.

79. Verhoeven, V.J., et al., Genome-wide meta-analyses of multiancestry cohorts identify multiple new susceptibility loci for refractive error and myopia. *Nat Genet*, 2013. **45**(3): 314-8.

80. Khawaja, A.P., et al., Genome-wide analyses identify 68 new loci associated with intraocular pressure and improve risk prediction for primary open-angle glaucoma. *Nat Genet*, 2018. **50**(6): 778-782.

81. Dreyer, S.D., et al., Mutations in LMX1B cause abnormal skeletal patterning and renal dysplasia in nail patella syndrome. *Nat Genet*, 1998. **19**(1): 47-50.

82. Bailey, J.N., et al., Genome-wide association analysis identifies TXNRD2, ATXN2 and FOXC1 as susceptibility loci for primary open-angle glaucoma. *Nat Genet*, 2016. **48**(2): 189-94.

Oculome version and run	Illumina Sequencing platform	Run Length	Number of samples	Cluster density K/mm^2		% passing filter (PF)	Total yield (Gb)	Coverage	Mean depth
				Lane 1	Lane 2				
Version 1 Pilot run	*MiSeq*	2 x 150 bp	8	1014*		87	4.8	96.0% > 30X	188X
Version 1 Run 1	*HiSeq2500*	2 x 100 bp	88	938	947	88.8	62.08	92.0% >30X	145 X
Version 2 Run 1	*HiSeq2500*	2 x 125 bp	64	848	852	94.9	74.75	99.5% >30X	234 X
Version 2 Run 2	*HiSeq2500*	2 x 125 bp	64	936	936	93.9	82.14	99.5% >30X	363 X
Version 2 Run 3	*HiSeq2500*	2 x 125 bp	64	938	947	93.0	82.0	99.0% >30X	324X
Version 2 Run 4	*NextSeq*	2 x 150 bp	64	142*		95.0	37.0	96.4% >30X	194X

***Table 1.** Run information for high-throughput sequencing runs in study performed on the Illumina MiSeq (Pilot Oculome 1) or Illumina HiSeq2500 using a rapid run mode flow cell. Oculome v2.1 to 2.3 showed improved coverage and mean read depth compared to early runs. PF = passing filter.*

Phenotypic Sub-group	No. Screened	No. Class 4/5 mutations	Diagnostic yield (%)
MAC	98	8	8.2
ASDA	113	28 (with 3 CNV)	24.8
RET	49	21	42.8
CAT	9	8	88.9
Syndromic and other	8	3 (with 1 CNV)	37.5
Total	277	68	**24.5%**

Table 2. Diagnostic yield (Clinical class 4/5)varied between 8.2% and 88.9% depending on the phenotype

Sample Number	Gene	Genotype	Sanger confirmation (Segregation analysis)	Mutation type (* previously reported as pathogenic)	cDNA	PROTEIN	MAF ExAc	PROTEIN DOMAIN	GENETIC DIAGNOSIS
12	*SMOC1*	COM HET	Yes. (M:p.Gln126His, F: c.379-2A>T)	Missense Splice site	c.378G>C c.379-2A>T	p.Gln126His p?	0	Thyroglobulin type-1	MIM: 206920
25	*ALDH1A3*	COM HET	Yes. (M:p.Asp292Tyr, F:p.Ile465Phe)	Missense Missense	c.553G>T c.1072A>T	p.Asp292Tyr p.Ile465Phe	0	Aldehyde dehydrogenase domain	MIM: 615113
112	*STRA6*	P COM HET	Yes. (M:p.Arg655His)	Missense* Nonsense	c.1964G>A c.1594 C>T	p.Arg655His p.Arg532*	T=0.00002 0	Inhibin, beta C subunit	MIM: 601186
190	*GDF3*	HET	Yes.(F:p.Arg266Cys)	Missense*	c.796C>T	p.Arg266Cys	A=0.0020	Transforming growth factor-beta, C-terminal	MIM: 613702
208	*GDF6*	HET	No	Missense*	c.746C>A	p.Ala249Glu	T=0.0010	Transforming growth factor-beta, N-terminal	MIM: 118100
260	*PRSS56*	HOM	No	Missense	c.320G>A	p.Gly107Glu	A=0.0013	Peptidase S1	MIM: 613517
294	*PORCN*	HET	Yes. (De novo)	Missense*	c.178G>A	p.Gly60Arg	0		MIM: 305600
10	*FOXC1*	HET	Yes. (De novo) No	Frameshift Missense	c.718_719delCT c.889C>T	p.Leu240Valfs*65 p.Pro297Ser	0 T=0.0022		MIM: 602482
127	*CYP1B1*	P COM HET	No	Missense Missense*	c.1139A>G c.182G>A	p.Tyr380Cys p.Gly61Glu*	0 T=0.0007	Cytochrome P450	MIM: 231300 or 617315
128	*CYP1B1*	P COM HET	No	Missense* Frameshift*	c.1103G>A c.1064_1076del	p.Arg368His p.Arg355Hisfs*69	T=0.0062 -=0.0002	Cytochrome P450	
136	*CYP1B1*	P COM HET	No	Missense* Missense	c.1103G>A c.290T>C	p.Arg368His p.Leu97Pro	T=0.0062	Cytochrome P450	
150	*CYP1B1*	COM HET	Yes. (M: p.Arg368His, F: p.Arg390His)	Missense* Missense*	c.1103G>A c.1169G>A	p.Arg368His p.Arg390His	T=0.0062	Cytochrome P450	
155	*CYP1B1*	HOM	No	Missense*	c.1103G>A	p.Arg368His	T=0.0062	Cytochrome P450	
159	*CYP1B1*	HOM	No	Nonsense*	c.171G>A	p.Trp57*	T=0.0004	Cytochrome P450	
167	*CYP1B1*	P COM HET	No	Frameshift* Frameshift Missense	c.868dupC c.862delinsCC c.317C>A	p.Arg290Profs*37 p.Ala288Profs*39 p.Ala106Asp	G=0.00005 0 T=0.00002		
177	*CYP1B1*	HOM	No	Frameshift	c.862delinsCC	p.Ala288Profs*39	0	Cytochrome P450	
180	*CYP1B1*	HOM	No	Missense*	c.1405C>T	p.Arg469Trp	A=0.00005	Cytochrome P450	
182	*CYP1B1*	P COM HET	No	Missense* Frameshift Frameshift	c.1159G>A c.749_750delins13 c.745_746delinsC	p.Glu387Lys p.Phe250Trpfs*4 p.Tyr249Profs*29	T=0.0003 0 0	Cytochrome P450	
226	*CYP1B1*	P COM HET	No	Missense Nonsense*	c.1147G>A c.171G>A	p.Ala383Thr p.Trp57*	0 T=0.0004	Cytochrome P450 Cytochrome P450	
54	*FOXC1*	HET	No	Nonsense	c.367C>T	p.Gln123*	0	Transcription factor, fork head	MIM: 601631 or 602482
67	*FOXC1*	HET	Yes (Both variants de novo)	Missense Missense	c.387C>A c.1239G>C	p.Asn129Lys p.Gln413His	0 0		

Sample Number	Gene	Genotype	Sanger confirmation (Segregation analysis)	Mutation type (* previously reported as pathogenic)	cDNA	PROTEIN	MAF ExAc	PROTEIN DOMAIN	GENETIC DIAGNOSIS
141	*FOXC1*	HET	No	Whole gene deletion*	chr6:1610653-1612371	p.?	NA	Transcription factor, fork head	
148	*FOXC1*	HET	No	Nonsense	c.75C>G	p.Tyr25*	0		
152	*FOXC1*	HET	No	Frameshift	c.1053_1056dup	p.Tyr353Argfs*176	0		
153	*FOXC1*	HET	No	Whole gene duplication*	chr6:1610653-1612371	p.?	0		
154	*FOXC1*	HET	No	Frameshift Frameshift	c.365_366insCT c.368_370delinsC	p.Trp122Cysfs*60 p.Gln123Profs*182	0		
162	*FOXC1*	HET	No	Nonsense	c.367C>T	p.Gln70*	0		
186	*FOXC1*	HET	Yes (No segregation)	Nonsense*	c.192C>T	p.Tyr64*	0		
264	*FOXC1*	HET	No	Whole gene deletion*	chr6:1610653-1612371	p.?	NA		
81	*FOXE3*	HET	Yes: (F, affected: p.*320Argext72)	Stop loss*	c.958T>C	p.*320Argext*72	0		MIM: 107250
205	*LTBP2*	HOM	No	Nonsense*	c.895C>T	Arg299Ter	A=0.00003		MIM: 613086
223	*TREX1*	HOM	No	Frameshift	c.628_631dup	p.Ala221Glyfs*2	0		MIM: 225750
236	*COL4A1*	HET	No	Missense*	c.2263G>A	p.Gly755Arg	0	Collagen triple helix repeat	MIM: 607595
241	*PAX6*	HET	No	Nonsense*	c.718C>T	p.Arg240*	0	Homeobox domain	MIM: 106210
322	*SLC4A11*	HOM	No	Missense*	c.2528T>C	p.Leu843Pro	G=0.000008		MIM: 217700 or 217400
74	*MYOC* *WDR36*	HET HET	Yes. (F:*MYOC*p.Gln368*, M:*WDR36* p.Asn355Ser)	Nonsense * Missense*	c.1102C>T c.1064A>G	p.Gln368* p.Asn355Ser	A=0.0011 G=0.0003	Olfactomedin-like	MIM: 137750 or 609887
89	*CNGA3*	HOM	Yes (Both parents heterozygous)	Missense*	c.1641C>A	p.Phe547Leu	A=0.0001	Cyclic nucleotide-binding domain	MIM: 216900
268	*CNGA3*	COM HET	Yes. (M: p.Ser419Phe, F:p.Gly584Arg)	Missense Missense	c.1256C>T c.1642G>A	p.Ser419Phe p.Gly548Arg	0 A=0.00002		
272	*CNGA3*	HOM	No	Missense*	c.1641C>A	p.Phe547Leu	A=0.0001		
278	*CNGA3*	COM HET	Yes. (M:p.Arg427Cys, F:p.Arg23*)	Missense* Nonsense*	c.1279C>T c.67C>T	p.Arg427Cys p.Arg23*	0 T=0.00002		
285	*CNGA3*	P COM HET	Yes (No segregation)	Missense* Missense	c.829C>T c.945C>G	p.Arg277Cys p.His315Gln	T=0.0001 0		
266	*CNGB3*	HOM	Yes (No segregation)	Frameshift*	c.1148del	p.Thr383Ilefs*13	-=0.0019		MIM: 262300 or 248200
271	*CNGB3*	P COM HET	Yes (No segregation)	Splice site* Frameshift*	c.1578+1G>A c.819_826del	p.? p.Arg274Valfs*13	T=0.00004 -=0.00003		
279	*CNGB3*	HOM	No	Frameshift*	c.1148del	p.Thr383Ilefs*13	-=0.0019		
333	*CNGB3*	P COM HET	Yes (M: c.1578+1G>A. F: p.Thr383Ilefs*13)	Splice site* Frameshift*	c.1578+1G>A c.1148del	p.? p.Thr383Ilefs*13	T=0.00004119 _=0.0019		

Sample Number	Gene	Genotype	Sanger confirmation (Segregation analysis)	Mutation type (* previously reported as pathogenic)	cDNA	PROTEIN	MAF ExAc	PROTEIN DOMAIN	GENETIC DIAGNOSIS
87	*ABCA4*	COM HET	Yes. M: p.Val2050Leu, p.Tyr1557Cys, F: p.Thr1526Met	Missense Missense Missense*	c.1648G>C c.4670A>G c.4577C>T	p.Val2050Leu p.Tyr1557Cys p.Thr1526Met	G=0.0028 0 A=0.00003	Rim ABC transporter	MIM: 248200, 601718 or 604116
91	*ABCA4*	HOM HOM	Yes: Both parents heterozygous for both variants	Missense* Missense*	c.3113C>T c.1622T>C	p.Ala1038Val p.Leu541Pro	A=0.0014 G=0.0001	Rim ABC transporter	
267	*ABCA4*	COM HET	Yes: F: p.Arg1108Cys, M: p.Arg152*	Missense* Nonsense*	c.3322G>A c.454G>A	p.Arg1108Cys p.Arg152*	A=0.0006 A=0.00008		
7	*RDH12*	HOM	Yes (both parents heterozygous)	Frameshift*	c.806_810del5	p.Ala269GlyfsTer2	0	Superfamily_domains: SSF51735	MIM: 612712
77	*CRB1*	P COM HET	No	Missense Splice site	c.2507G>A c.3670-1G>A	p.Cys836Tyr p.?	A=0.0002 unknown		MIM: 600105, 613835
88	*COL2A1*	HET	Yes (F, affected: p.Arg565Cys)	Missense*	c.1693C>T	p.Arg565Cys	0		MIM: 108300 or 609508
90	*GUCY2D*	HOM	No	Missense	c.1996C>T	p.Arg666Trp	T=0.00000824	Serine-threonine/tyrosine-protein kinase catalytic domain	MIM: 204000
261	*RPE65*	COM HET	Yes (M:p.Gly484Asp, F: p.Tyr249Cys)	Missense* Missense	c.1451G>A c.746A>G	p.Gly484Asp p.Tyr249Cys	T=0.00002 C=0.00004	Carotenoid oxygenase Carotenoid oxygenase	MIM: 204100 or 613794
	PDE6B[a]	HET	Yes (Both from unaffected mother)	Nonsense Missense	c.2401C>T c.173C>T	p.Gln801* p.Ala58Val	T=0.00002 T=0.00005	3'5'-cyclic nucleotide phosphodiesterase, catalytic domain	MIM: 613801 or 163500
269	*CACNA1F*	HEMIZ	No	Nonsense*	c.148G>A	p.Arg50*8	0		MIM: 300071, 300600 or 300476
	RAX2	HET	No	Frameshift	c.473C>CG	p.Leu114Alafs*18	0		MIM: 610381
274	*CACNA1F*	HEMIZ	Yes (No segregation)	Frameshift	c.3492dup	p.Lys1165Glnfs*18	0		MIM: 300071, 300600 or 300476
273	*TSPAN12*	HOM	No	Splice site	c.361-2A>G	p.?	0		MIM: 613310 (recessive forms reported)
325	*PROM1*	HET	No	Missense*	c.1117C>T	p.Arg373Cys	0	Prominin	MIM: 608051
71	*CRYAA*	HET	No	Missense*	c.34C>T	p.Arg12Cys	0	Alpha-crystallin, N-terminal	MIM: 123580
287	*CRYAA*	HET	No	Missense	c.275A>G	p.Asp92Gly	0	Heat shock protein Hsp20	MIM: 123580
191	*CRYGD*	HET	No	Missense*	c.70C>A	p.Pro24Thr	0	Beta/gamma crystallin	MIM: 115700
290	*CRYGD*	HET	No	Nonsense	c.418C>T	p.Arg140*	0	Beta/gamma crystallin	MIM: 115700
96	*MAF*	HET	No	Missense	c.892A>T	p.Asn298Tyr	0	Basic leucine zipper domain, Maf-type	MIM: 610202

Sample Number	Gene	Genotype	Sanger confirmation (Segregation analysis)	Mutation type (* previously reported as pathogenic)	cDNA	PROTEIN	MAF ExAc	PROTEIN DOMAIN	GENETIC DIAGNOSIS
187	*CRYBA1*	HET	No	Nonsense	c.528T>G	p.Tyr176*	0	Beta/gamma crystallin	MIM: 600881
288	*GJA8*	HET	No	Missense	c.77T>C	p.Leu26Pro	0	Connexin, N-terminal	MIM: 600897
289	*EPHA2**	HET	No	Splice region*	c.2826-9G>A	p.?	0		MIM: 116600
251	*OCA2*	P COM HET	No No	Missense* Deletion of Exon 7*	c.2228C>T chr15:28263504-28263742 deletion	p.Pro743Leu p.?	0.0000906 NA	Divalent ion symporter	MIM: 203200
59	*SRD5A3*	HOM	No	Nonsense*	c.57G>A	p.Trp19*	A=0.0001179		MIM: 612379 or 612713
60	*SRD5A3*	HOM	No	Nonsense*	c.57G>A	p.Trp19*	A=0.0001179		MIM: 612379 or 612713
Incidental Findings									
68	*TGFBI*	HET	No	Missense	c.1998G>C	Arg666Ser	C=0.0016	TGF beta-induced protein bIGH3/osteoblast-specific factor 2	MIM: 121820
141	*VSX1*	HET	No	Missense	c.479G>A	p.Gly160Asp	T=0.0021		

Table 3. ***Likely pathogenic or known pathogenic variants (Clinical class 4 or 5)****. All class 4 or 5 variant detected in the study subdivided by sub-panel (Pink: MAC, Green: ASDA, Yellow: Retinal Dystrophies, Blue: Congenital cataracts, Grey: Oculocutaneous albinism and others). Clinical diagnosis following mutation analysis is given in column 'Diagnosis'. 61 diagnoses were made out of 254 cases analysed. 25 had dominant variantss and 35 had recessive variants (homozygous or compound heterozygous), and 1 case composite. Minor allele frequencies (MAF) were extracted from ExAc (http://exac.broadinstitute.org/), which includes genetic variation derived from 60,706 unrelated individuals. Exact breakpoints ofr structural variants could not be mapped. The extent of structural variants shown in this table indicate the overlap of the structural variant with our target region. [a] This variant was inherited from the apparently asymptomatic mother but may modify the phenotype. [b] This variant is outside the splice site but is a previously reported pathogenic variant. M: Mother, F: Father*

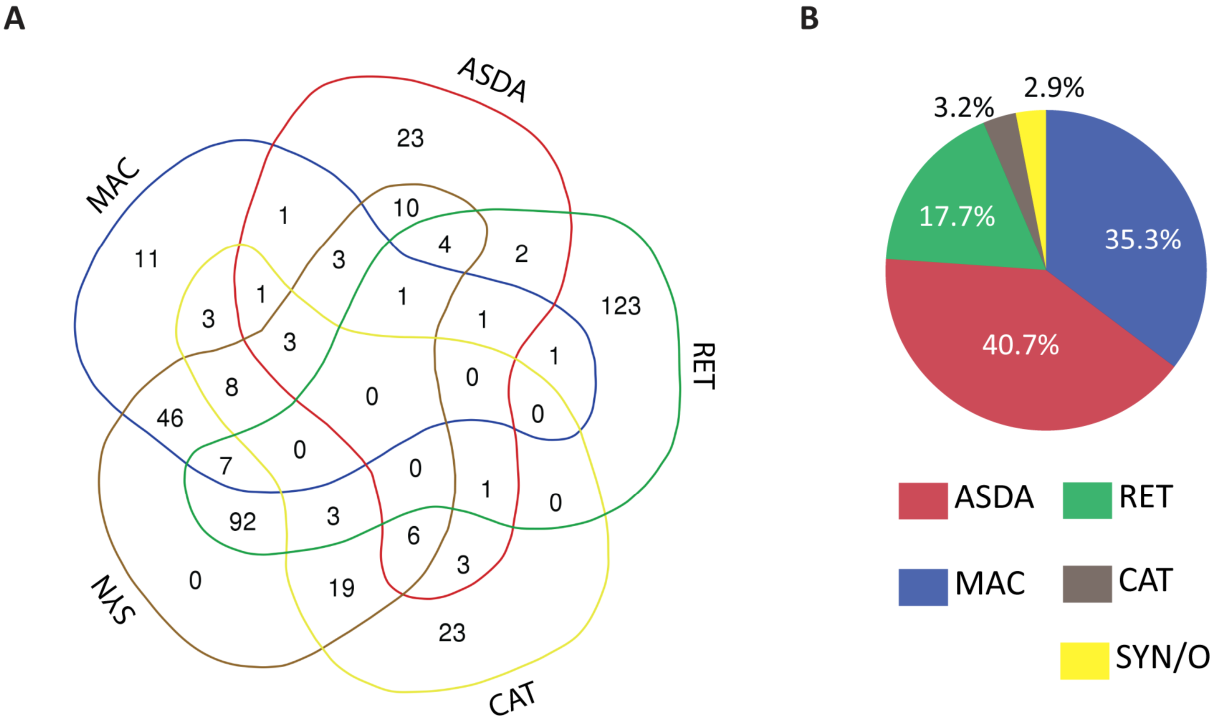
A
MAC
ASDA
RET
CAT
SYN
23
11
1
10
3
4
2
3
1
1
123
3
1
3
8
0
0
1
46
0
7
0
0
1
0
92
3
6
3
0
19
23
B
2.9%
3.2%
17.7%
35.3%
40.7%
ASDA
RET
MAC
CAT
SYN/O

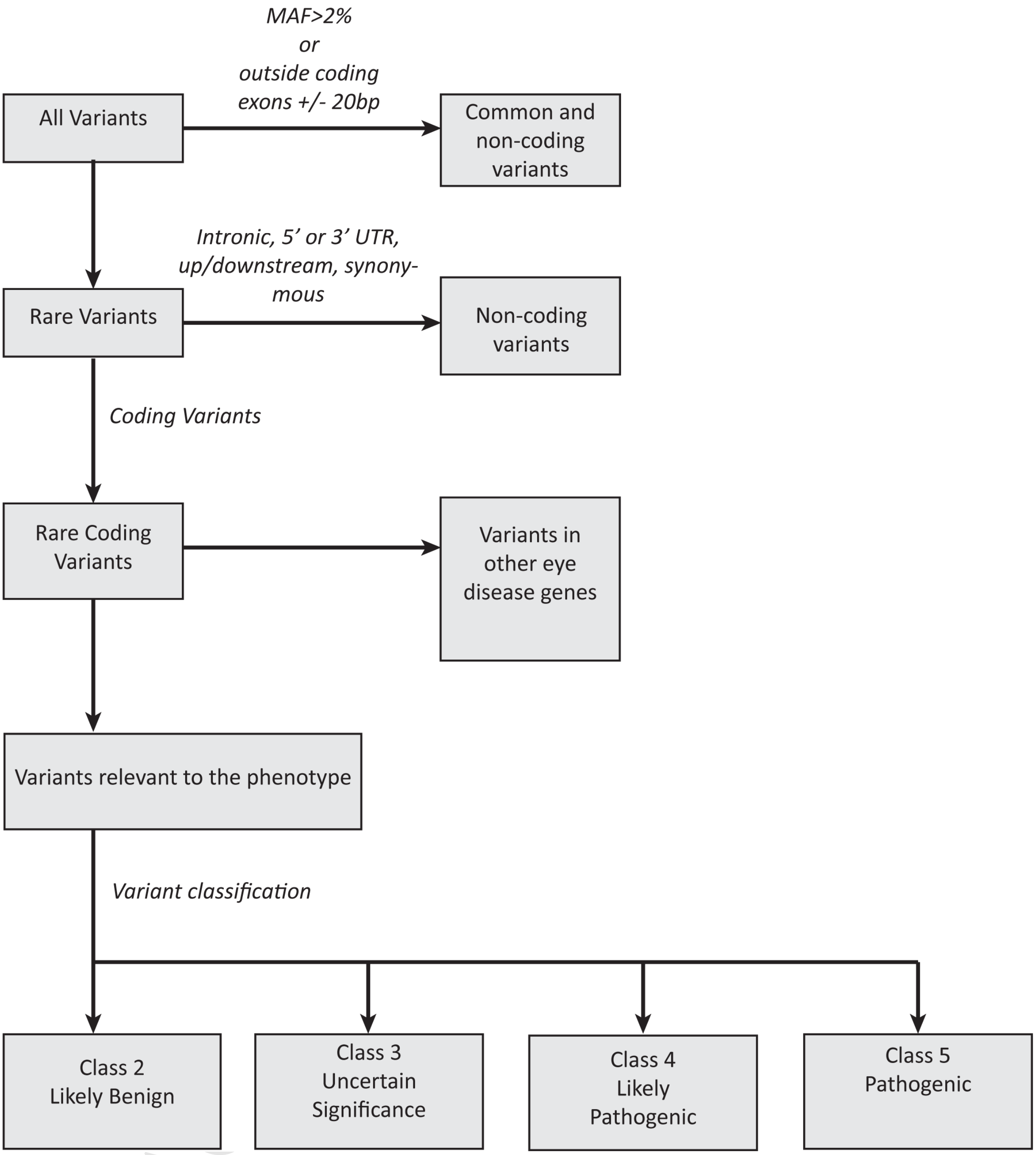
MAF>2%
or
outside coding
exons +/- 20bp
All Variants
Common and non-coding variants
Intronic, 5’ or 3’ UTR, up/downstream, synonymous
Rare Variants
Non-coding variants
Coding Variants
Rare Coding Variants
Variants in other eye disease genes
Variants relevant to the phenotype
Variant classification
Class 2
Likely Benign
Class 3
Uncertain Significance
Class 4
Likely Pathogenic
Class 5
Pathogenic

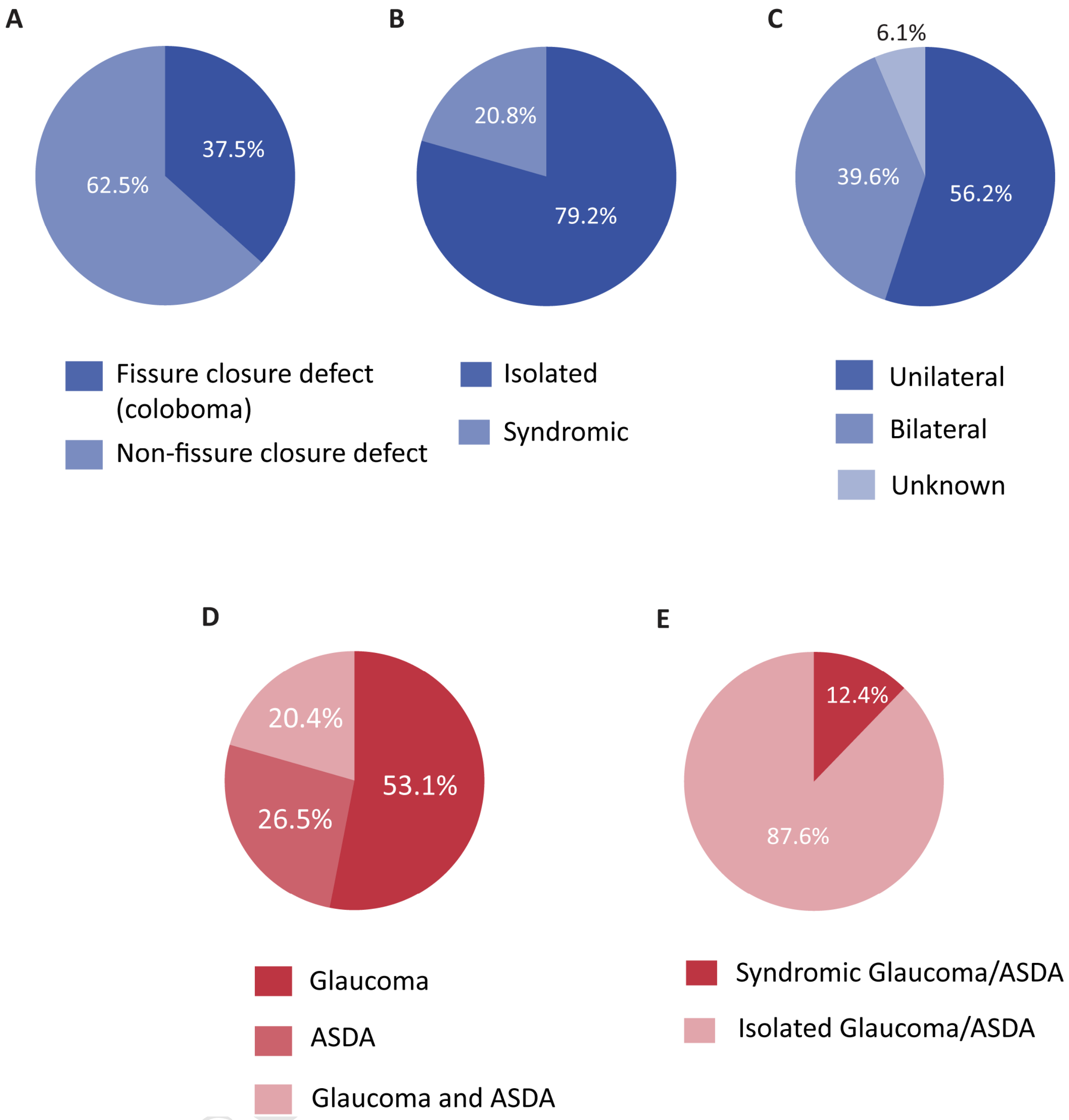
A
37.5%
62.5%
Fissure closure defect (coloboma)
Non-fissure closure defect
B
20.8%
79.2%
Isolated
Syndromic
C
6.1%
39.6%
56.2%
Unilateral
Bilateral
Unknown
D
20.4%
53.1%
26.5%
Glaucoma
ASDA
Glaucoma and ASDA
E
12.4%
87.6%
Syndromic Glaucoma/ASDA
Isolated Glaucoma/ASDA

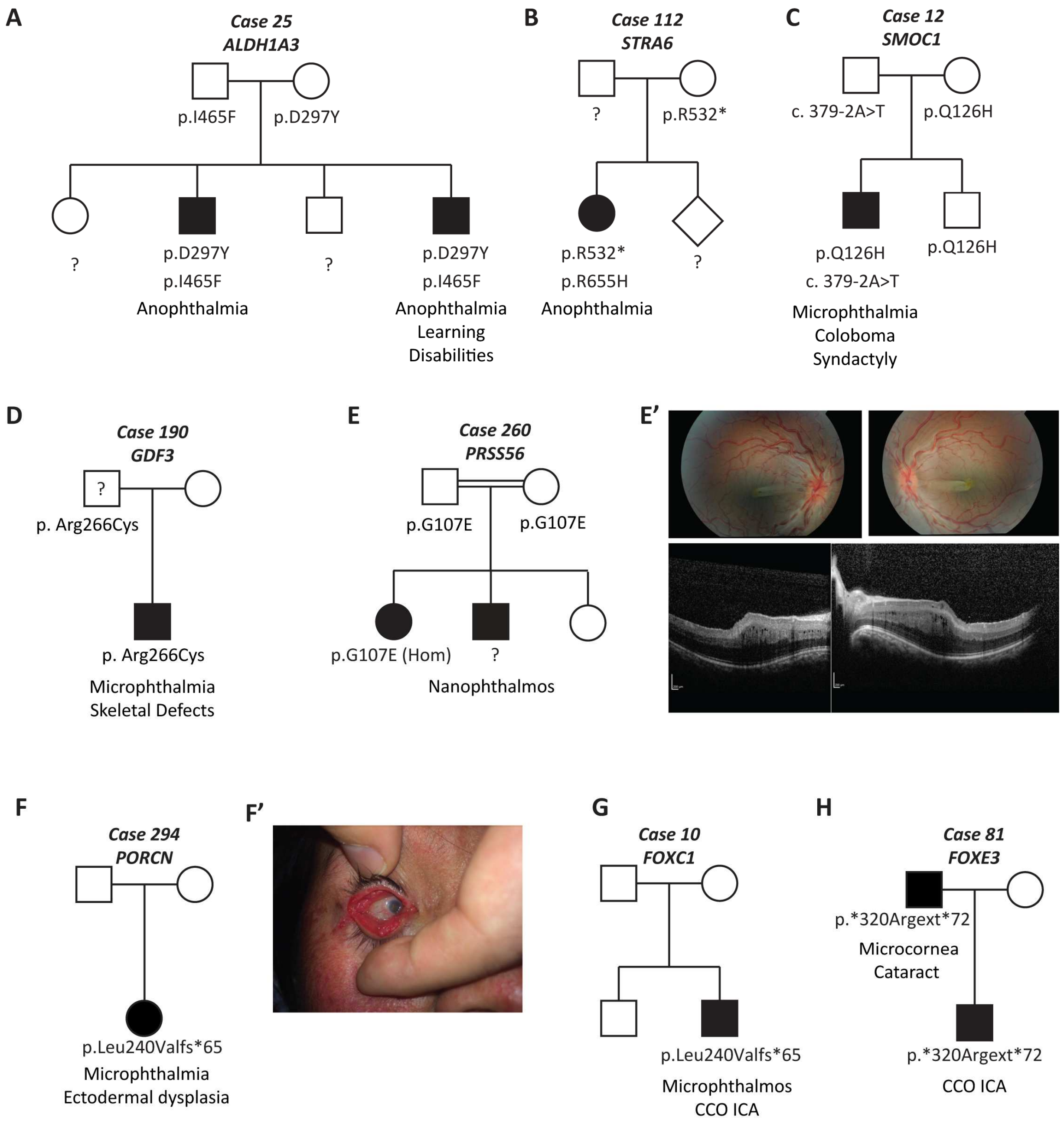
A
Case 25
ALDH1A3
p.I465F
p.D297Y
?
p.D297Y
p.I465F
Anophthalmia
?
p.D297Y
p.I465F
Anophthalmia
Learning
Disabilities
B
Case 112
STRA6
?
p.R532*
p.R532*
p.R655H
Anophthalmia
?
C
Case 12
SMOC1
c. 379-2A>T
p.Q126H
p.Q126H
c. 379-2A>T
Microphthalmia
Coloboma
Syndactyly
p.Q126H
D
Case 190
GDF3
?
p. Arg266Cys
p. Arg266Cys
Microphthalmia
Skeletal Defects
E
Case 260
PRSS56
p.G107E
p.G107E
p.G107E (Hom)
?
Nanophthalmos
E’
F
Case 294
PORCN
p.Leu240Valfs*65
Microphthalmia
Ectodermal dysplasia
F’
G
Case 10
FOXC1
p.Leu240Valfs*65
Microphthalmos
CCO ICA
H
Case 81
FOXE3
p.*320Argext*72
Microcornea
Cataract
p.*320Argext*72
CCO ICA

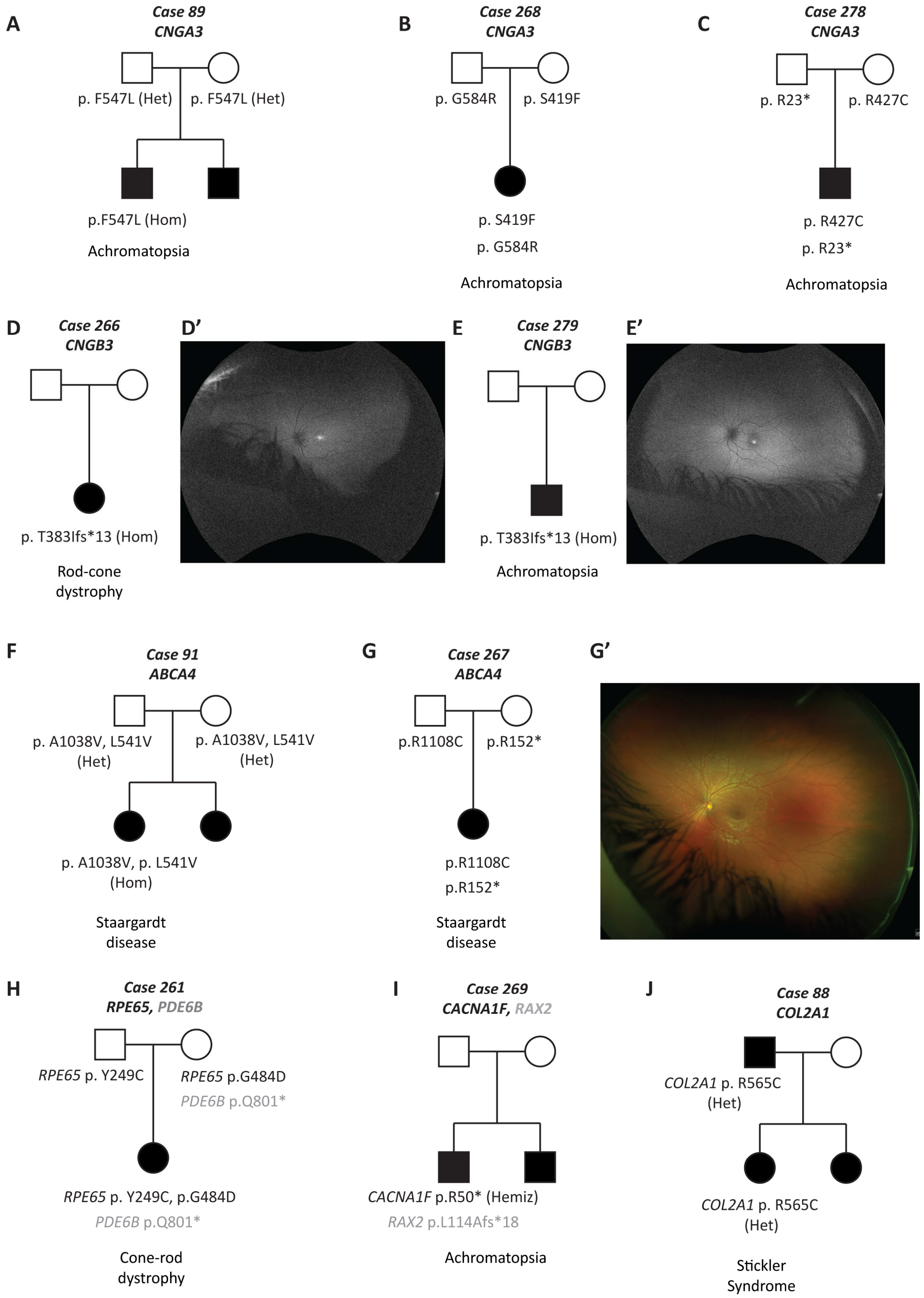
A
Case 89
CNGA3
p. F547L (Het)
p. F547L (Het)
p.F547L (Hom)
Achromatopsia
B
Case 268
CNGA3
p. G584R
p. S419F
p. S419F
p. G584R
Achromatopsia
C
Case 278
CNGA3
p. R23*
p. R427C
p. R427C
p. R23*
Achromatopsia
D
Case 266
CNGB3
p. T383Ifs*13 (Hom)
Rod-cone dystrophy
D’
E
Case 279
CNGB3
p. T383Ifs*13 (Hom)
Achromatopsia
E’
F
Case 91
ABCA4
p. A1038V, L541V (Het)
p. A1038V, L541V (Het)
p. A1038V, p. L541V (Hom)
Staargardt disease
G
Case 267
ABCA4
p.R1108C
p.R152*
p.R1108C
p.R152*
Staargardt disease
G’
H
Case 261
RPE65, PDE6B
RPE65 p. Y249C
RPE65 p.G484D
PDE6B p.Q801*
RPE65 p. Y249C, p.G484D
PDE6B p.Q801*
Cone-rod dystrophy
I
Case 269
CACNA1F, RAX2
CACNA1F p.R50* (Hemiz)
RAX2 p.L114Afs*18
Achromatopsia
J
Case 88
COL2A1
COL2A1 p. R565C (Het)
COL2A1 p. R565C (Het)
Stickler Syndrome

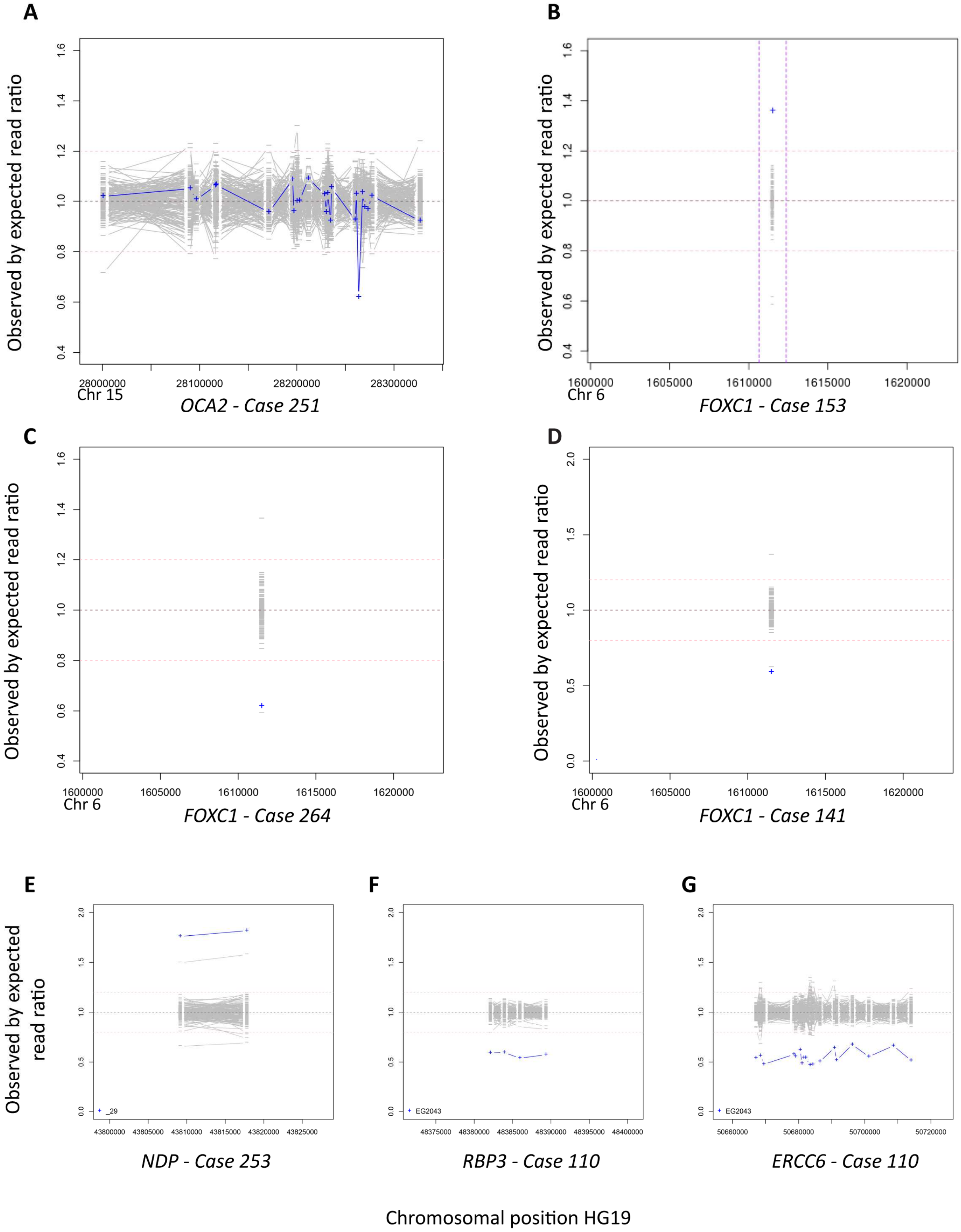
A
Observed by expected read ratio
0.4
0.6
0.8
1.0
1.2
1.4
1.6
28000000
28100000
28200000
28300000
Chr 15
OCA2 - Case 251
B
Observed by expected read ratio
1600000
1605000
1610000
1615000
1620000
Chr 6
FOXC1 - Case 153
C
Observed by expected read ratio
1600000
1605000
1610000
1615000
1620000
Chr 6
FOXC1 - Case 264
D
Observed by expected read ratio
0.0
0.5
1.0
1.5
2.0
1600000
1605000
1610000
1615000
1620000
Chr 6
FOXC1 - Case 141
E
Observed by expected read ratio
_29
43800000
43805000
43810000
43815000
43820000
43825000
NDP - Case 253
F
EG2043
48375000
48380000
48385000
48390000
48395000
48400000
RBP3 - Case 110
G
EG2043
50660000
50680000
50700000
50720000
ERCC6 - Case 110
Chromosomal position HG19

Title

The Oculome panel test: next-generation sequencing to diagnose a diverse range of genetic developmental eye disorders

Running Title

Genetic testing of developmental eye disorders

Highlights

To address the challenge of heterogeneity of developmental eye diseases we developed the oculome test, screening 429 genes. Evaluation in a cohort with varied congenital eye conditions revealed variability in diagnostic yields between phenotypic subgroups.